CHAPTER

15

FLOW OVER BODIES: DRAG AND LIFT

I n Chap. 14, we considered the flow of fluids inside pipes, with emphasis on pressure drop and head losses and their relations to flow rate. In this chapter, we consider the flow of fluids over bodies that are immersed in a fluid, called *external flow*, with emphasis on the resulting lift and drag forces. External flow is characterized by a freely growing boundary layer surrounded by an outer flow region that involves small velocity and temperature gradients.

In internal flows, the entire flow field is dominated by viscous effects, while in external flow, the viscous effects are confined to a portion of flow field such as the boundary layers and waters.

When a fluid moves over a solid body, it exerts pressure forces normal to the surface and shear forces parallel to the surface along the outer surface of the body. We are usually interested in the *resultant* of the pressure and shear forces acting on the body rather than the details of the distributions of these forces along the entire surface of the body. The component of the resultant pressure and shear forces that acts in the flow direction is called the *drag force,* and the component that acts normal to the flow direction is called the *lift.*

We start this chapter with a discussion of drag and lift and explore the concepts of pressure drag, friction drag, and flow separation. We continue with the drag coefficients of various two- and three-dimensional geometries encountered in practice and determine the drag force using experimentally determined drag coefficients. We then examine the development of the velocity boundary layer during parallel flow over a flat surface, and develop relations for the skin friction coefficient for flow over flat plates, cylinders, and spheres. Finally, we discuss the lift developed by airfoils and the factors that affect the lift characteristics of bodies.

CONTENTS

15–1 ▪ INTRODUCTION

Fluid flow over solid bodies frequently occurs in practice, and it is responsible for numerous physical phenomena such as the *drag force* acting on automobiles, power lines, trees, and underwater pipelines; the *lift* developed by airplane wings; *upward draft* of rain, snow, hail, and dust particles in high winds; the transportation of red blood cells by blood flow; the entrainment and disbursement of liquid droplets by sprays; the vibration and noise generated by bodies moving in a fluid; and the power generated by wind turbines (Fig. 15–1). Therefore, developing a good understanding of external flow is important in the design of many engineering systems such as aircraft, automobiles, buildings, ships, submarines, and all kinds of turbines. Late-model cars, for example, have been designed with particular emphasis on aerodynamics. This has resulted in significant reductions in fuel consumption and noise, and considerable improvement in handling.
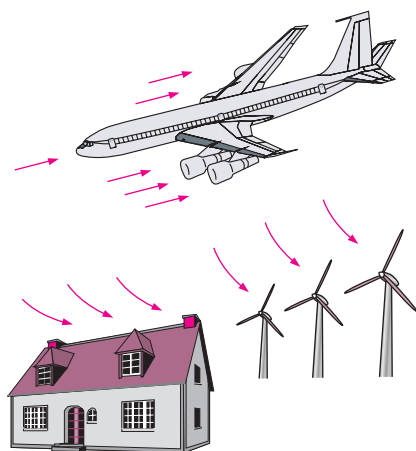
Sometimes a fluid moves over a stationary body (such as the wind blowing over a building), and other times a body moves through a quiescent fluid (such as a car moving through air). These two seemingly different processes are equivalent to each other; what matters is the relative motion between the fluid and the body. Such motions are conveniently analyzed by fixing the coordinate system on the body and are referred to as **flow over bodies** or **external flow.** The aerodynamic aspects of different airplane wing designs, for example, are studied conveniently in a lab by placing the wings in a wind tunnel and blowing air over them by large fans.

The flow fields and geometries for most external flow problems are too complicated to be solved analytically, and thus we have to rely on correlations based on experimental data. The availability of high-speed computers has made it possible to conduct series of "numerical experimentations" quickly by solving the governing equations numerically, and to resort to the expensive and time-consuming testing and experimentation only in the final stages of design. Such testing is done in wind tunnels. H. F. Phillips (1845–1912) built the first wind tunnel in 1894 and measured lift and drag. In this chapter we will mostly rely on relations developed experimentally.

The velocity of the fluid approaching a body is called the **free-stream velocity,** and is denoted by $\mathcal{V}$. It is also denoted by u_∞ or U_∞ when the flow is aligned with the x-axis since u is used to denote the x-component of velocity. The fluid velocity ranges from zero at the surface (the no-slip condition) to the free-stream value away from the surface, and the subscript "infinity" serves as a reminder that this is the value at a distance where the presence of the body is not felt. The free-stream velocity may vary with location and time (e.g., the wind blowing past a building). But in the design and analysis, the free-stream velocity is usually assumed to be *uniform* and *steady* for convenience, and this is what we will do in this chapter.

The shape of a body has a profound influence on the flow over the body and the velocity field. The flow over a body is said to be **two-dimensional** when the body is very long and of constant cross section and the flow is normal to the body. The wind blowing over a long pipe perpendicular to its axis is an example of two-dimensional flow. Note that the velocity component in the axial direction is zero in this case, and thus the velocity is two-dimensional.

FIGURE 15–1
Flow past bodies is commonly encountered in practice.

The two-dimensional idealization is appropriate when the body is sufficiently long so that the end effects are negligible and the approach flow is uniform. Another simplification occurs when the body possesses symmetry along an axis in the flow direction. The flow in this case is also two-dimensional and is said to be **axisymmetric.** A bullet piercing through air is an example of axisymmetric flow. The velocity in this case varies with the axial distance x and the radial distance r. Flow over a body that cannot be modeled as two-dimensional or axisymmetric such as flow over a car is **three-dimensional** (Fig. 15–2).

Flow over bodies can also be classified as **incompressible flows** (e.g., flows over automobiles, submarines, and buildings) and **compressible flows** (e.g., flows over high-speed aircraft, rockets, and missiles). Compressibility effects are negligible at velocities below about 100 m/s (or 360 km/h), and such flows can be treated as incompressible. Compressible flow and flows that involve partially immersed bodies with a free surface (such as a ship cruising in water) are beyond the scope of this introductory text.

Bodies subjected to fluid flow are classified as being streamlined or blunt, depending on their overall shape. A body is said to be **streamlined** if a conscious effort is made to align its shape with the anticipated streamlines in the flow. Streamlined bodies such as race cars and airplanes appear to be contoured and sleek. Otherwise, a body (such as a building) tends to block the flow and is said to be **bluff** or **blunt.** Usually it is much easier to force a streamlined body through a fluid, and thus streamlining has been of great importance in the design of vehicles and airplanes (Fig. 15–3).

Variations in velocity during internal or external flow, in general, are accompanied by changes in pressure in accordance with the Bernoulli equation (when the viscous effects are negligible). For liquid flow, the pressure at some points may drop below the vapor pressure of the liquid, causing the liquid to vaporize or "boil" at those locations and to form small vapor bubbles, called *cavitation bubbles* (see Chap. 10). At 15°C, for example, the vapor pressure of water is 1.7 kPa. Therefore, water may cavitate at locations where the pressure drops below this value (due to high velocities) such as in the constrictions in a valve or the tips of impeller blades.
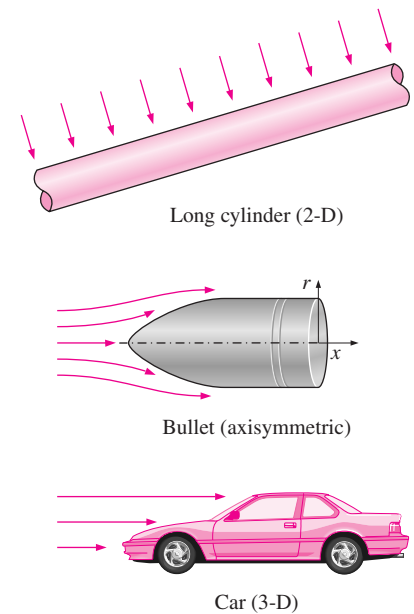
15–2 DRAG AND LIFT

It is a common experience that a body meets some resistance when it is forced to move through a fluid, especially a liquid. As you may have noticed, it is very difficult to walk in water because of the much greater resistance it offers
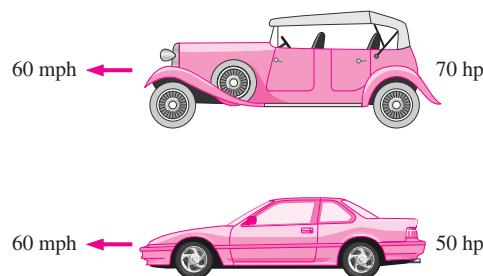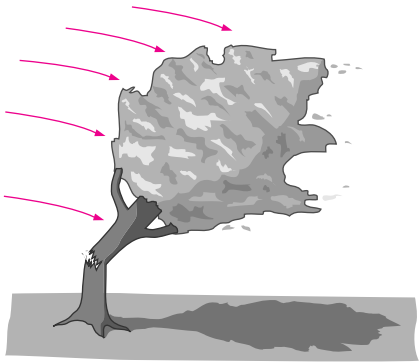
FIGURE 15–2
Two-dimensional, axisymmetric, and three-dimensional flows.

FIGURE 15–3
Usually it is much easier to force a streamlined body than a blunt body through a fluid.

FIGURE 15–4
High winds knock down trees, power lines, and even people as a result of the drag force.

to motion compared to air. Also, you may have seen high winds knocking down trees, power lines, and even trailers and felt the strong "push" the wind exerts on your body (Fig. 15–4). You experience the same feeling when you extend your arm out of the window of a moving car. A fluid may exert forces and moments on a body in and about various directions. The force a flowing fluid exerts on a body in the flow direction is called **drag.** The drag force can be measured directly by simply attaching the body subjected to fluid flow to a calibrated spring and measuring the displacement in the flow direction (just like measuring weight with a spring scale). More sophisticated drag-measuring devices, called drag balances, use flexible beams fitted with strain gages to measure the drag electronically.

Drag is usually an undesirable effect, like friction, and we do our best to minimize it. Reduction of drag is closely associated with the reduction of fuel consumption in automobiles, submarines, and aircraft; improved safety and durability of structures subjected to high winds; and reduction of noise and vibration. But in some cases drag produces a very beneficial effect and we try to maximize it. Friction, for example, is a "life saver" in the brakes of automobiles. Likewise, it is the drag that makes it possible for people to parachute, for pollens to fly to distant locations, and for us all to enjoy the waves of the oceans and the relaxing movements of the leaves of trees.

A stationary fluid exerts only normal pressure forces on the surface of a body immersed in it. A moving fluid, however, also exerts tangential shear forces on the surface because of the no-slip condition caused by viscous effects. Both of these forces, in general, have components in the direction of flow, and thus the drag force is due to the combined effects of pressure and wall shear forces in the flow direction. The components of the pressure and wall shear forces in the direction normal to the flow tend to move the body in that direction, and their sum is called **lift.**

For two-dimensional flows, the resultant of the pressure and shear forces can be split into two components: one in the direction of flow, which is the drag force, and another in the direction normal to flow, which is the lift, as shown in Fig. 15–5. For three-dimensional flows, there is also a side force component in the direction normal to page that tends to move the body in that direction.

The fluid forces also may generate moments and cause the body to rotate. The moment about the flow direction is called the *rolling moment,* the

FIGURE 15–5
The pressure and viscous forces acting on a two-dimensional body and the resultant lift and drag forces.

$$F_D = F_R \cos \alpha$$
$$F_L = F_R \sin \alpha$$
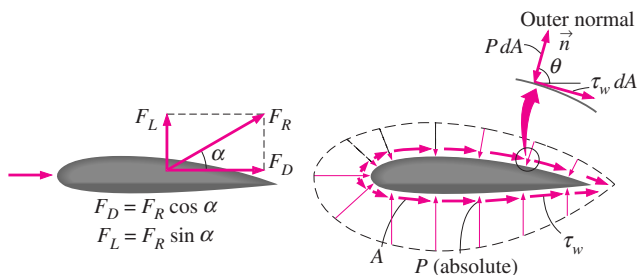
moment about the lift direction is called the *yawing moment,* and the moment about the side force direction is called the *pitching moment.* For bodies that possess symmetry about the lift-drag plane such as cars, airplanes, and ships, the side force, the yawing moment, and the rolling moment are zero when the wind and wave forces are aligned with the body. What remain for such bodies are the drag and lift forces and the pitching moment. For axisymmetric bodies aligned with the flow, such as a bullet, the only force exerted by the fluid on the body is the drag force.

The pressure and shear forces acting on a differential area *dA* on the surface are *PdA* and $\tau_w dA,$ respectively. The differential drag force and the lift force acting on *dA* in two-dimensional flow are (Fig. 15–5)

$$dF_D = -P\,dA\,\cos\theta + \tau_w\,dA\,\sin\theta \qquad \textbf{(15–1)}$$

and

$$dF_L = -P\,dA\,\sin\theta - \tau_w\,dA\,\cos\theta \qquad \textbf{(15–2)}$$

where θ is the angle the outer normal of *dA* makes with the positive flow direction. The total drag and lift acting on the body can be determined by integrating the last relations over the entire surface of the body,

Drag force: $\qquad F_D = \int_A dF_D = \int_A (-P\cos\theta + \tau_w \sin\theta)\,dA \qquad \textbf{(15–3)}$

and

Lift force: $\qquad F_L = \int_A dF_L = -\int_A (P\sin\theta + \tau_w \cos\theta)\,dA \qquad \textbf{(15–4)}$

These are the equations used to predict the net drag and lift forces on bodies when the flow is simulated on a computer. However, when we perform experimental analyses, Eqs. 15–3 and 15–4 are not practical since the detailed distributions of pressure and shear forces are difficult to obtain by measurements. Fortunately, this information is often not needed. Usually all we need to know is the resultant drag force and lift acting on the entire body, which can be measured directly and easily in a wind tunnel.

Equations 15–1 and 15–2 show that both the skin friction (wall shear) and pressure, in general, contribute to the drag and the lift. In the special case of a thin *flat plate* aligned parallel to the flow direction, the drag force depends on the wall shear only and is independent of pressure since $\theta = 90°$. When the flat plate is placed normal to the flow direction, however, the drag force depends on the pressure only and is independent of wall shear since the shear stress in this case acts in the direction normal to flow and $\theta = 0°$ (Fig. 15–6). If the flat plate is tilted at an angle θ relative to the flow direction, then the drag force depends on both the pressure and the shear stress.

The wings of airplanes are shaped and positioned specifically to generate lift with minimal drag. This is done by maintaining an angle of attack during
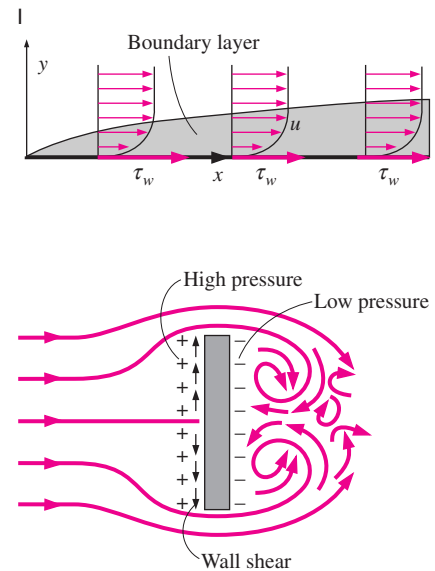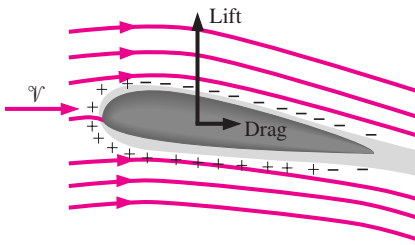

FIGURE 15–6
Drag force acting on a flat plate parallel to flow depends on wall shear only (top); drag force acting on a flat plate normal to flow depends on the pressure only and is independent of the wall shear, which acts normal to flow (bottom).

FIGURE 15–7
Airplane wings are shaped and positioned to generate sufficient lift during flight while keeping drag at a minimum.

cruising, as shown in Fig. 15–7. Both lift and drag are strong functions of the angle of attack, as we discuss later. The pressure difference between the top and bottom surfaces of the wing generates an upward force that tends to lift the wing and thus the airplane to which it is connected. For slender bodies such as wings, the shear force acts nearly parallel to the flow direction, and thus its contribution to the lift is small. The drag force for such slender bodies is mostly due to shear forces (the skin friction).

The drag and lift forces depend on the density ρ of the fluid, the upstream velocity $\mathcal{V}$, and the size, shape, and orientation of the body, among other things, and it is not practical to list these forces for a variety of situations. Instead, it is found convenient to work with appropriate dimensionless numbers that represent the drag and lift characteristics of the body. These numbers are the **drag coefficient** C_D, and the **lift coefficient** C_L, and they are defined as

Drag coefficient:
$$C_D = \frac{F_D}{\frac{1}{2}\rho \mathcal{V}^2 A} \tag{15–5}$$

Lift coefficient:
$$C_L = \frac{F_L}{\frac{1}{2}\rho \mathcal{V}^2 A} \tag{15–6}$$

where A is ordinarily the **frontal area** (the area projected on a plane normal to the direction of flow) of the body. In other words, A is the area that would be seen by a person looking at the body from the direction of the approaching fluid. The frontal area of a cylinder of diameter D and length L, for example, is $A = LD$. In lift calculations of some bodies, such as airfoils, A is taken to be the **planform area,** which is the area seen by a person looking at the body from above in a direction normal to the body. The drag and lift coefficients are primarily functions of the shape of the body, but in some cases they also depend on the Reynolds number and the surface roughness. The term $\frac{1}{2}\rho \mathcal{V}^2$ is the **dynamic pressure.**

The local drag and lift coefficients vary along the surface as a result of the changes in the velocity boundary layer in the flow direction. We are usually interested in the drag and lift forces for the *entire* surface, which can be determined using the *average* drag and lift coefficients. Therefore, we present correlations for both local (identified with the subscript x) and average drag and lift coefficients. When relations for local drag and lift coefficients for a surface of length L are available, the *average* drag and lift coefficients for the entire surface can be determined by integration from

$$C_D = \frac{1}{L}\int_0^L C_{D,x}\, dx \tag{15–7}$$

and

$$C_L = \frac{1}{L}\int_0^L C_{L,x}\, dx \tag{15–8}$$

When a body is dropped into the atmosphere or a lake, it first accelerates under the influence of its weight. The motion of the body is resisted by the drag force, which acts in the direction opposite to motion. As the velocity of the body increases, so does the drag force. This continues until all the forces balance each other and the net force acting on the body (and thus its acceleration) is zero. Then the velocity of the body remains constant during the rest of its fall if the properties of the fluid in the path of the body remain essentially constant. This is the maximum velocity a falling body can attain and is called the **terminal velocity** (Fig. 15–8). The forces acting on a falling body are usually the drag force, the buoyant force, and the weight of the body.
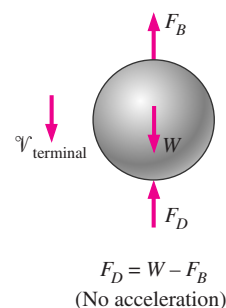

$$F_D = W - F_B$$
(No acceleration)

FIGURE 15–8
During a free fall, a body reaches its *terminal velocity* when the drag force equals the weight of the body minus the buoyant force.
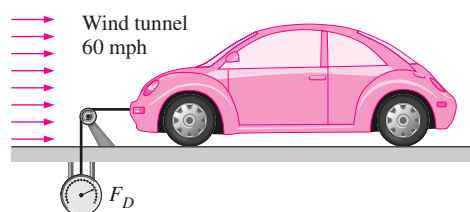
EXAMPLE 15–1   Measuring the Drag Coefficient of a Car

The drag coefficient of a car at the design conditions of 1 atm, 70°F, and 60 mph is to be determined experimentally in a large wind tunnel in a full-scale testing. The height and width of the car are 4.2 ft and 5.3 ft, respectively (Fig. 15–9). If the force acting on the car in the flow direction is measured to be 68 lbf, determine the drag coefficient of this car.

SOLUTION   The drag force acting on a car is measured in a wind tunnel. The drag coefficient of the car at the test conditions is to be determined.
Assumptions   **1** The flow of air is steady and incompressible. **2** The cross section of the tunnel is large enough to simulate free flow over the car. **3** The bottom of the tunnel is also moving at the speed of air to approximate actual driving conditions or this effect is negligible.
Properties   The density of air at 1 atm and 70°F is $\rho = 0.07489$ lbm/ft³ (Table A–22E).
Analysis   The drag force acting on a body and the drag coefficient are given by

$$F_D = C_D A \frac{\rho \mathcal{V}^2}{2} \qquad \text{and} \qquad C_D = \frac{2F_D}{\rho A \mathcal{V}^2}$$

Wind tunnel
60 mph

F_D

FIGURE 15–9
Schematic for Example 15–1.

where A is the frontal area. Substituting and noting that 1 mph = 1.467 ft/s, the drag coefficient of the car is determined to be

$$C_D = \frac{2 \times (68\text{ lbf})}{(0.07489\text{ lbm/ft}^3)(4.2 \times 5.3\text{ ft}^2)(60 \times 1.467\text{ ft/s})^2}\left(\frac{32.2\text{ lbm} \cdot \text{ft/s}^2}{1\text{ lbf}}\right) = \mathbf{0.34}$$

Discussion   Note that the drag coefficient depends on the design conditions, and its value may be different at different conditions. Therefore, the published drag coefficients of different vehicles can be compared meaningfully only if they are determined under similar conditions. This shows the importance of developing standard testing procedures in industry.

15–3 ▪ FRICTION AND PRESSURE DRAG

As mentioned earlier, the drag force is the net force exerted by a fluid on a body in the direction of flow due to the combined effects of wall shear and pressure forces. It is often instructive to separate the two effects, and study them separately.

The part of drag that is due directly to wall shear stress τ_w is called the **skin friction drag** (or just *friction drag $F_{D,\text{ friction}}$*) since it is caused by frictional effects, and the part that is due directly to pressure P is called the **pressure drag** (also called the *form drag* because of its strong dependence on the form or shape of the body). The friction and pressure drag coefficients are defined as

$$C_{D,\text{ friction}} = \frac{F_{D,\text{ friction}}}{\frac{1}{2}\rho V^2 A} \qquad \text{and} \qquad C_{D,\text{ pressure}} = \frac{F_{D,\text{ pressure}}}{\frac{1}{2}\rho V^2 A} \qquad \textbf{(15–9)}$$

When the friction and pressure drag coefficients or forces are available, the total drag coefficient or drag force can be determined by simply adding them,

$$C_D = C_{D,\text{ friction}} + C_{D,\text{ pressure}} \qquad \text{and} \qquad F_D = F_{D,\text{ friction}} + F_{D,\text{ pressure}} \qquad \textbf{(15–10)}$$

The *friction drag* is the component of the wall shear force in the direction of flow, and thus it depends on the orientation of the body as well as the magnitude of the wall shear stress τ_w. The friction drag is *zero* for a flat surface normal to flow, and *maximum* for a flat surface parallel to flow since the friction drag in this case equals the total shear force on the surface. Therefore, for parallel flow over a flat surface, the drag coefficient is equal to the *friction drag coefficient,* or simply the *friction coefficient*. Friction drag is a strong function of viscosity, and increases with increasing viscosity.

The Reynolds number is inversely proportional to the viscosity of the fluid. Therefore, the contribution of friction drag to total drag for blunt bodies is less at higher Reynolds numbers, and may be negligible at very high Reynolds numbers. The drag in such cases is mostly due to pressure drag. At low Reynolds numbers, most drag is due to friction drag. This is especially the case for highly streamlined bodies such as airfoils. The friction drag is also proportional to the surface area. Therefore, bodies with a larger surface area experiences a larger friction drag. Large commercial airplanes, for example,
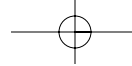
reduce their total surface area and thus their drag by retracting their wing extensions when they reach cruising altitudes to save fuel. The friction drag coefficient is independent of *surface roughness* in laminar flow, but is a strong function of surface roughness in turbulent flow due to surface roughness elements protruding further into the viscous sublayer. The *friction drag coefficient* is analogous to the *friction factor* in pipe flow discussed in Chap. 14, and its value depends on the flow regime.

The pressure drag is proportional to the frontal area, and to the *difference* between the pressures acting on the front and back of the immersed body. Therefore, the pressure drag is usually dominant for blunt bodies, negligible for streamlined bodies such as airfoils, and zero for thin flat plates parallel to the flow (Fig. 15–10). The pressure drag becomes most significant when the velocity of the fluid is too high for the fluid to be able to follow the curvature of the body, and thus the fluid *separates* from the body at some point and creates a very low pressure region in the back. The pressure drag in this case is due to the large pressure difference between the front and back sides of the body.

Reducing Drag by Streamlining

The first thought that comes to mind to reduce drag is to streamline a body in order to reduce flow separation and thus to reduce pressure drag. Even car salesmen are quick to point out the low drag coefficients of their cars, owing to streamlining. But streamlining has opposite effects on pressure and friction drags. It decreases pressure drag by delaying boundary layer separation and thus reducing the pressure difference between the front and back of the body and increases the friction drag by increasing the surface area. The end result depends on which effect dominates. Therefore, any optimization study to reduce the drag of a body must consider both effects and must attempt to minimize the *sum* of the two, as shown in Fig. 15–11. The minimum total drag occurs at $D/L = 0.25$ for the case shown in Fig. 15–11. For the case of a circular cylinder with the same thickness as the streamlined shape of Fig. 15–11, the drag coefficient would be about five times as much. Therefore, it is possible to reduce the drag of a cylindrical component to one-fifth by the use of proper fairings.
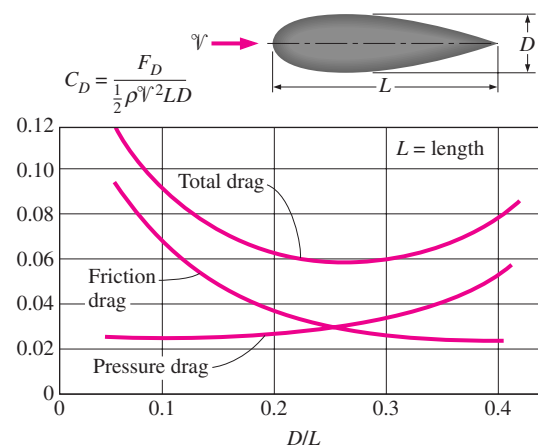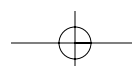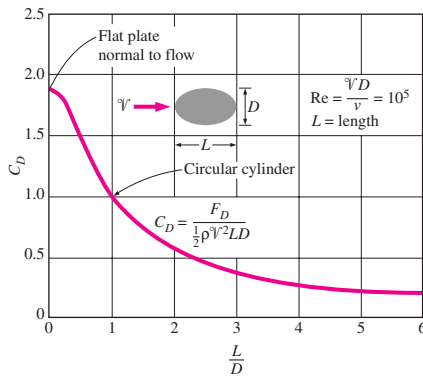

FIGURE 15–10
Drag is due entirely to *friction drag* for a flat plate parallel to flow; it is due entirely to pressure drag for a flat plate normal to flow; and it is due to *both* (but mostly *pressure drag*) for a cylinder normal to flow. The total drag coefficient C_D is lowest for a parallel flat plate, highest for a vertical flat plate, and in between (but close to that of a vertical flat plate) for a cylinder. (from G. M. Homsy, et al.)

FIGURE 15–11
The variation of friction, pressure, and total drag coefficients of a streamlined strut with thickness-to-chord length ratio for $Re = 4 \times 10^4$ (from Abbott and von Doenhoff).

$$C_D = \frac{F_D}{\frac{1}{2}\rho \mathcal{V}^2 LD}$$

L = length

Total drag

Friction drag

Pressure drag

D/L

FIGURE 15–12
The variation of the drag coefficient of a long elliptical cylinder with aspect ratio based on the frontal area bD (from Blevins).

The effect of streamlining on the drag coefficient can be described best by considering long elliptical cylinders with different aspect (or length-to-width) ratios L/D, where L is the length in the flow direction and D is the thickness, as shown in Fig. 15–12. Note that the drag coefficient decreases drastically as the ellipse becomes slimmer. For the special case of $L/D = 1$ (a circular cylinder), the drag coefficient is $C_D \approx 1$ at this Reynolds number. As the aspect ratio is decreased and the cylinder resembles a flat plate, the drag coefficient increases to 1.9, the value for a flat plate normal to flow. Note that the curve becomes nearly flat for aspect ratios greater than about 4. Therefore, for a given diameter D, elliptical shapes with an aspect ratio of about $L/D \approx 4$ usually offer good compromise between the total drag coefficient and length L. The reduction in the drag coefficient at high aspect ratios is primarily due to the boundary layer staying attached to the surface longer and the resulting pressure recovery. The friction drag on an elliptical cylinder with an aspect ratio of 4 is negligible (less than 2 percent of total drag).

As the aspect ratio of an elliptical cylinder is increased by flattening it (i.e., decreasing D while holding L constant), the drag coefficient starts increasing and tends to infinity as $L/D \to \infty$ (i.e., as the ellipse resembles a flat plate parallel to flow). This is due to the frontal area, which appears in the denominator in the definition of C_D, approaching zero. It does not mean that the drag force increases drastically (actually, the drag force decreases) as the body becomes flat. This shows that the frontal area is inappropriate for use in the drag force relations for slim bodies such as thin airfoils and flat plates. In such cases, the drag coefficient is defined on the basis of the *planform area,* which is simply the surface area for a flat plate. This is quite appropriate since for slim bodies the drag is almost entirely due to friction drag, which is proportional to the surface area.

Streamlining has the added benefit of *reducing vibration and noise.* Streamlining should be considered only for blunt bodies that are subjected to high-velocity fluid flow (and thus high Reynolds numbers) for which flow separation is a real possibility. It is not necessary for bodies that typically involve low Reynolds number flows (e.g., creeping flows in which Re < 1, since the drag in those cases is almost entirely due to friction drag, and streamlining will only increase the surface area and thus the total drag. Therefore, careless streamlining may actually increase drag instead of decreasing it.
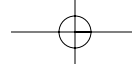
Flow Separation

When driving on country roads, it is a common safety measure to slow down at sharp turns in order to avoid being thrown off the road. Many drivers have learned the hard way that a car will refuse to comply when forced to turn curves at excessive speeds. We can view this phenomenon as "the separation of cars" from the roads. This phenomenon is also observed when fast vehicles jump off hills. At low velocities, the wheels of the vehicle always remain in contact with the road surface. But at high velocities, the vehicle is too fast to follow the curvature of the road and takes off at the hill, losing contact with the road.

A fluid acts the same way when forced to flow over a curved surface at high velocities. A fluid climbs the uphill portion of the curved surface with no problem, but it has difficulty remaining attached to the surface on the downhill side. At sufficiently high velocities, the fluid stream detaches itself from the surface of the body. This is called **flow separation** (Fig. 15–13). Flow can
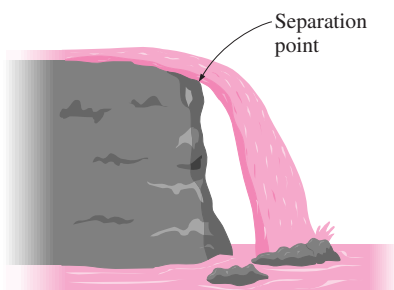
FIGURE 15–13
Flow separation in a waterfall.

separate from a surface even if it is fully submerged in a liquid or immersed in a gas (Fig. 15–14). The location of the separation point depends on several factors such as the Reynolds number, the surface roughness, and the level of fluctuations in the free stream, and it is usually difficult to predict exactly where separation will occur, unless there are sharp corners or abrupt changes in the shape of the solid surface.

When a fluid separates from a body, it forms a separated region between the body and the fluid stream. This low pressure region behind the body where re-circulating and back flows occur is called the **separated region.** The larger the separated region, the larger the pressure drag. The effects of flow separation are felt far downstream in the form of reduced velocity (relative to the up-stream velocity). The region of flow trailing the body where the effects of the body on velocity are felt is called the **wake** (Fig. 15–15). The separated region comes to an end when the two flow streams reattach. Therefore, the separated region is an enclosed volume, whereas the wake keeps growing behind the body until the fluid in the wake region regains its velocity and the velocity profile becomes nearly flat again. Viscous and rotational effects are the most significant in the boundary layer, the separated region, and the wake. The flow outside these regions can be considered to be irrotational.

The occurrence of separation is not limited to blunt bodies. Separation may also occur on a streamlined body such as an airplane wing at a sufficiently large **angle of attack** (larger than about 16° for most airfoils), which is the angle the incoming fluid stream makes with the **chord** (the line that connects the nose and the end) of the body. Flow separation on the top surface of a wing reduces lift drastically and may cause the airplane to **stall.** Stalling has been blamed for many airplane accidents and loss of efficiencies in turbomachinery (Fig. 15–16).

Note that drag and lift are strongly dependent on the shape of the body, and any effect that causes the shape to change has a profound effect on the drag and lift. For example, snow accumulation and ice formation on airplane wings may change the shape of the wings sufficiently to cause significant loss of lift. This phenomenon has caused many airplanes to lose altitude and crash and many others to abort takeoff. Therefore, it has become a routine safety measure to check for ice or snow buildup on critical components of airplanes before takeoff in bad weather. This is especially important for airplanes that have waited a long time on the runway before takeoff because of heavy traffic.
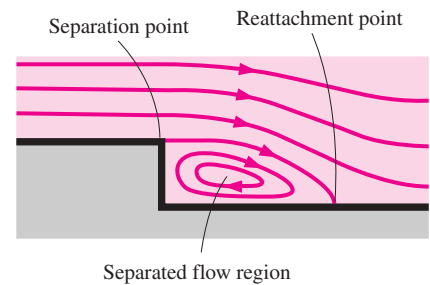

FIGURE 15–14
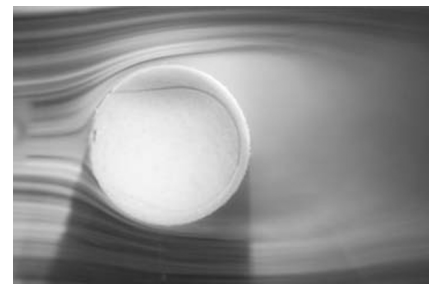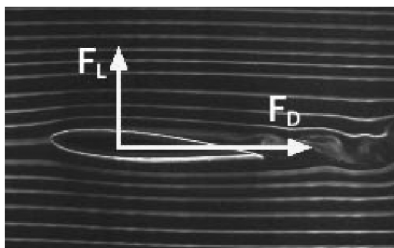Flow separation over a backward-facing step along a wall.
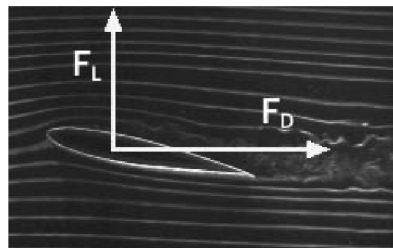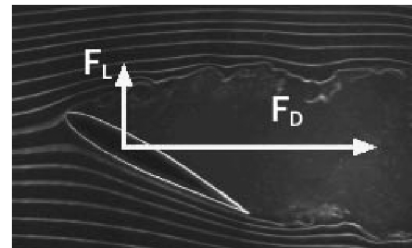

FIGURE 15–15
Flow separation during flow over a tennis ball, and the wake region. (Courtesy NASA and Cislunar Aerospace, Inc.)
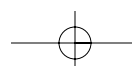

(*a*) 5°   (*b*) 15°   (*c*) 30°

FIGURE 15–16
At large angles of attack (usually larger than 15°), flow may separate completely from the top surface of an airfoil, reducing lift drastically and causing the airfoil to stall. (from G. M. Homsy, et al.)

An important consequence of flow separation is the formation and shedding of circulating fluid chunks, called **vortices,** in the wake region. The continual generation of these vortices downstream is referred to as **vortex shedding.** This phenomenon usually occurs during normal flow over long cylinders or spheres for Re $\geq$ 90. The vibrations generated by vortices near the body may cause the body to resonate to dangerous levels if the frequency of the vortices is close to the natural frequency of the body—a situation that must be avoided in the design of equipment that is subjected to high-velocity fluid flow such as the wings of airplanes and suspended bridges subjected to steady high winds.

15–4 ▪ DRAG COEFFICIENTS OF COMMON GEOMETRIES

The concept of drag has important consequences in daily life, and the drag behavior of various natural and man-made bodies is characterized by their drag coefficients measured under typical operating conditions. Although drag is caused by two different effects (friction and pressure), it is usually difficult to determine them separately. Besides, in most cases, we are interested in the *total* drag rather than the individual drag components, and thus usually the *total* drag coefficient is reported. The determination of drag coefficients has been the topic of numerous studies (mostly experimental), and there is a huge amount of drag coefficient data in the literature for just about any geometry of practical interest.

The drag coefficient, in general, depends on the *Reynolds number,* especially for Reynolds numbers below about 10^4. At higher Reynolds numbers, the drag coefficients for most geometries remain essentially constant (Fig. 15–17). This is due to the flow at high Reynolds numbers becoming fully turbulent. However, this is not the case for rounded bodies such as circular cylinders and spheres, as we discuss later. The reported drag coefficients are usually applicable only to flows at high Reynolds numbers.

The drag coefficient exhibits different behavior in the low (creeping), moderate (laminar), and high (turbulent) regions of Reynolds number. The inertia effects are negligible in low Reynolds number flows (Re $<$ 1), called **creeping flows,** and the fluid wraps around the body smoothly. The drag coefficient
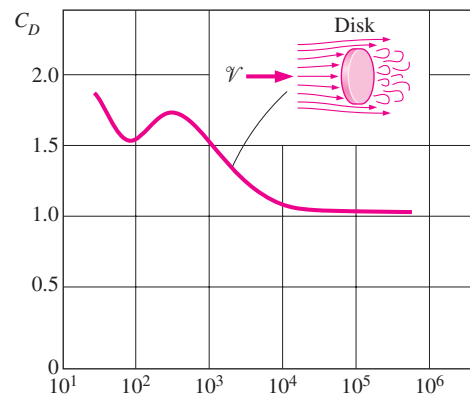
FIGURE 15–17
The drag coefficients for most geometries (but not all) remain essentially constant at Reynolds numbers above about 10^4.
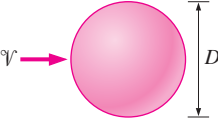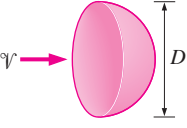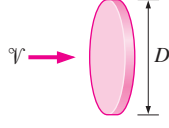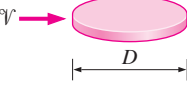
Sphere	Hemisphere
$\mathcal{V} \rightarrow$ D	$\mathcal{V} \rightarrow$ D
$C_D = 24/\text{Re}$	$C_D = 22.2/\text{Re}$

Circular disk (normal to flow)	Circular disk (parallel to flow)
$\mathcal{V} \rightarrow$ D	$\mathcal{V} \rightarrow$ D
$C_D = 20.4/\text{Re}$	$C_D = 13.6/\text{Re}$

FIGURE 15–18
Drag coefficients C_D at low velocities (Re ≤ 1 where Re = $\mathcal{V}D/\upsilon$ and $A = \pi D^2/4$).

in this case is inversely proportional to the Reynolds number, and for a sphere it is determined to be

Sphere:
$$C_D = \frac{24}{\text{Re}} \qquad (\text{Re} \leqslant 1) \qquad \qquad \textbf{(15–11)}$$

Then the drag force acting on a spherical object at low Reynolds numbers becomes

$$F_D = C_D A \frac{\rho \mathcal{V}^2}{2} = \frac{24}{\text{Re}} A \frac{\rho \mathcal{V}^2}{2} = \frac{24}{\rho \mathcal{V} D/\mu} \frac{\pi D^2}{4} \frac{\rho \mathcal{V}^2}{2} = 3\pi\mu\mathcal{V}D \qquad \textbf{(15–12)}$$

which is known as **Stokes law,** after British mathematician and physicist G. G. Stokes (1819–1903). This relation shows that at very low Reynolds numbers, the drag force acting on spherical objects is proportional to the diameter, the velocity, and the viscosity of the fluid. This relation is often applicable to dust particles in the air and suspended solid particles in water.

The drag coefficients for low Reynolds number flows past some other geometries are given in Fig. 15–18. Note that at low Reynolds numbers, the shape of the body does not have a major influence on the drag coefficient.

The drag coefficients for various two- and three-dimensional bodies are given in Tables 15–1 and 15–2 for large Reynolds numbers. We can make several observations from these tables about the drag coefficient at high Reynolds numbers. First of all, the *orientation* of the body relative to the direction of flow has a major influence on the drag coefficient. For example, the drag coefficient for flow over a hemisphere is 0.4 when the spherical side faces the flow, but it increases threefold to 1.2 when the flat side faces the flow (Fig. 15–19). This shows that the rounded nose of a *bullet* serves another purpose in addition to piercing: reducing drag and thus increasing the range of the gun.

For blunt bodies with sharp corners, such as flow over a rectangular block or a flat plate normal to flow, separation occurs at the edges of the front and
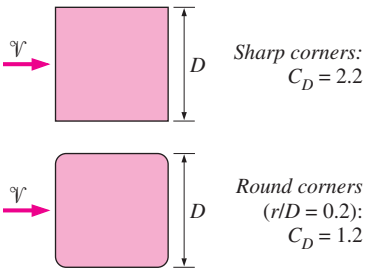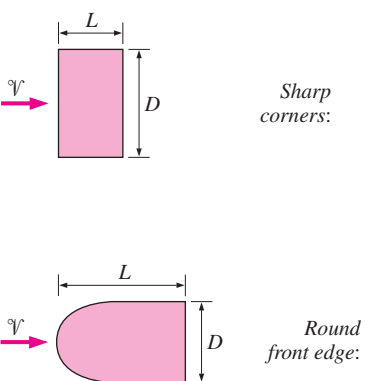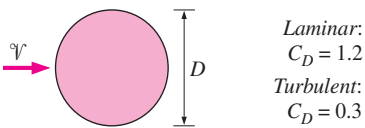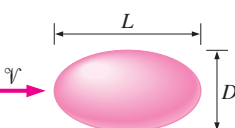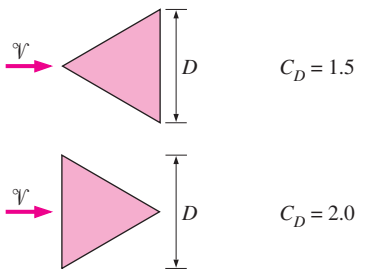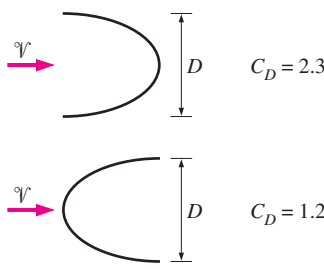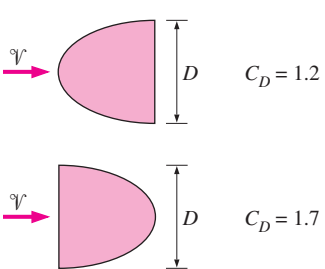
A hemisphere at two different orientations for Re > 10^4

$\mathcal{V} \rightarrow$ $C_D = 0.4$

$\mathcal{V} \rightarrow$ $C_D = 1.2$
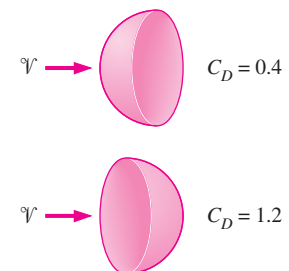
FIGURE 15–19
The drag coefficient of a body may change drastically by changing its orientation (and thus shape) relative to the direction of flow.

TABLE 15–1

Drag coefficients C_D of various two-dimensional bodies for Re $> 10^4$ based on the frontal area $A = bD$, where b is the length in direction normal to paper (for use in the drag force relation $F_D = C_D A \rho V^2/2$ where V is the upstream velocity)

Square rod

$V \rightarrow \square \, D$ *Sharp corners:* $C_D = 2.2$

$V \rightarrow \square \, D$ *Round corners* $(r/D = 0.2)$: $C_D = 1.2$

Rectangular rod

$V \rightarrow \square \, D$ L *Sharp corners:*

L/D	C_D
0.0*	1.9
0.1	1.9
0.5	2.5
1.0	2.2
2.0	1.7
3.0	1.3

*Corresponds to thin plate

$V \rightarrow \; D$ L *Round front edge:*

L/D	C_D
0.5	1.2
1.0	0.9
2.0	0.7
4.0	0.7

Circular rod (cylinder)

$V \rightarrow \bigcirc \, D$ *Laminar:* $C_D = 1.2$ *Turbulent:* $C_D = 0.3$

Elliptical rod

$V \rightarrow \; L \; D$

L/D	C_D	
	Laminar	Turbulent
2	0.60	0.20
4	0.35	0.15
8	0.25	0.10

Equilateral triangular rod

$V \rightarrow \triangleleft \, D$ $C_D = 1.5$

$V \rightarrow \triangleright \, D$ $C_D = 2.0$

Semicircular shell

$V \rightarrow \; D$ $C_D = 2.3$

$V \rightarrow \; D$ $C_D = 1.2$

Semicircular rod

$V \rightarrow \; D$ $C_D = 1.2$

$V \rightarrow \; D$ $C_D = 1.7$
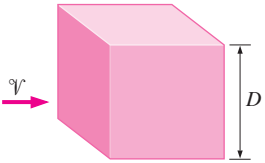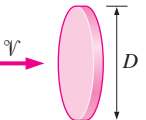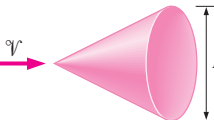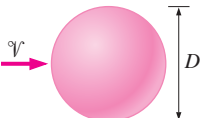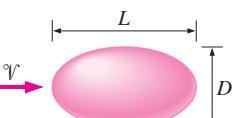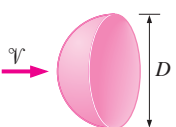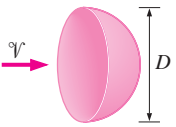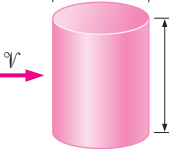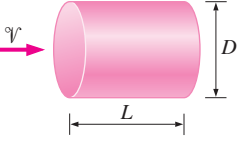
back surfaces, with no significant change in the character of flow. Therefore, the drag coefficient of such bodies is nearly independent of the Reynolds number. Note that the drag coefficient of a long rectangular rod can be reduced almost by half from 2.2 to 1.2 by rounding the corners.

Biological Systems and Drag

The concept of drag also has important consequences for biological systems. For example, the bodies of *fish,* especially the ones that swim fast for long distances (such as dolphins), are highly streamlined to minimize drag (the drag

TABLE 15–2

Representative drag coefficients C_D for various three-dimensional bodies for Re $> 10^4$ based on the frontal area (for use in the drag force relation $F_D = C_D A\rho \mathcal{V}^2/2$ where $\mathcal{V}$ is the upstream velocity)

Cube, $A = D^2$	Thin circular disk, $A = \pi D^2/4$	Cone (for $\theta = 30°$), $A = \pi D^2/4$
$C_D = 1.05$	$C_D = 1.1$	$C_D = 0.5$

Sphere, $A = \pi D^2/4$	Ellipsoid, $A = \pi D^2/4$			
Laminar: $C_D = 0.5$ Turbulent: $C_D = 0.2$				C_D

L/D	Laminar	Turbulent
0.75	0.5	0.2
1	0.5	0.2
2	0.3	0.1
4	0.3	0.1
8	0.2	0.1

Hemisphere, $A = \pi D^2/4$	Short cylinder, vertical, $A = L/D$	Short cylinder, horizontal, $A = \pi D^2/4$
$C_D = 0.4$ $C_D = 1.2$		

Short cylinder, vertical:

L/D	C_D
1	0.6
2	0.7
5	0.8
10	0.9

Short cylinder, horizontal:

L/D	C_D
0.5	1.1
1	0.9
2	0.9
4	0.9
8	1.0

(continued)

coefficient of dolphins based on the wetted skin area is about 0.0035, comparable to the value for a flat plate in turbulent flow). So it is no surprise that we build submarines that mimic large fish. Tropical fish with fascinating beauty and elegance, on the other hand, swim gracefully short distances only. Obviously grace, not high speed and drag, was the primary consideration in their design. Birds teach us a lesson on drag reduction by extending their beak forward and folding their feet backward during flight (Fig. 15–20). Airplanes, which look somewhat like big birds, retract their wheels after takeoff in order to reduce drag and thus fuel consumption.

The flexible structure of plants enables them to reduce drag at high winds by changing their shapes. Large flat leaves, for example, curl into a low-drag conical shape at high wind speeds, while tree branches cluster to reduce drag. Flexible trunks bend under the influence of the wind to reduce drag, and the bending moment is lowered by reducing frontal area.

If you watch the Olympic games, you have probably observed many instances of conscious effort by the competitors to reduce drag. Some examples:
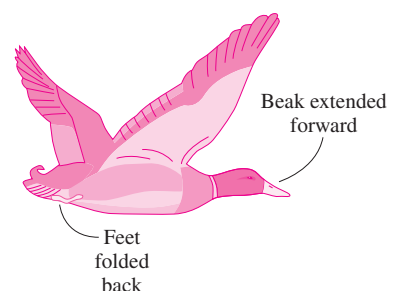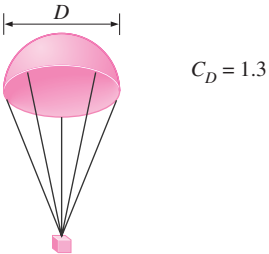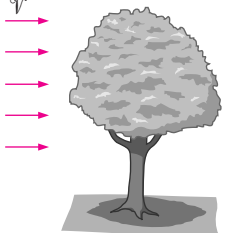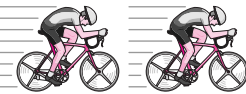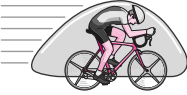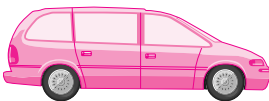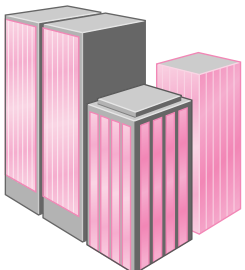
FIGURE 15–20
Birds teach us a lesson on drag reduction by extending their beak forward and folding their feet backward during flight.

TABLE 15–2 (*Concluded*)

Streamlined body, $A = \pi D^2/4$	Parachute, $A = \pi D^2/4$	Tree, A = frontal area
$\mathcal{V}$ D $C_D = 0.04$	$C_D = 1.3$	$\mathcal{V}$, m/s $\quad$ C_D 10 $\quad$ 0.4–1.2 20 $\quad$ 0.3–1.0 30 $\quad$ 0.2–0.7

Person (average)	Bikes
Standing, $C_D A = 9\ \text{ft}^2 = 0.84\ \text{m}^2$ Sitting, $C_D A = 6\ \text{ft}^2 = 0.56\ \text{m}^2$	Upright: $A = 5.5\ \text{ft}^2 = 0.51\ \text{m}^2$ $C_D = 1.1$ $\qquad$ Drafting: $A = 3.9\ \text{ft}^2 = 0.36\ \text{m}^2$ $C_D = 0.50$ Racing: $A = 3.9\ \text{ft}^2 = 0.36\ \text{m}^2$ $C_D = 0.9$ $\qquad$ With fairing: $A = 5.0\ \text{ft}^2 = 0.46\ \text{m}^2$ $C_D = 0.12$

Semitruck (A = frontal area)	Automotive (A = frontal area)	High-rise buildings (A = frontal area)
Without fairing: $C_D = 0.96$ With fairing: $C_D = 0.76$	Minivan, $C_D = 0.4$ Passenger car, $C_D = 0.3$	$C_D = 1.4$

During 100-m running, the runners hold their fingers together and straight and move their hands parallel to the direction of motion to reduce the drag on their hands. Swimmers with long hair cover their head with a tight and smooth cover to reduce head drag. They also wear well-fitting one-piece swimming suits. Horse and bicycle riders lean forward as much as they can to reduce drag (by reducing both the drag coefficient and frontal area). Speed skiers do the same thing. Fairings are commonly used in motorcycles to reduce drag.

Drag Coefficients of Vehicles

The term *drag coefficient* is commonly used in various areas of daily life. Car manufacturers try to attract consumers by pointing out the *low drag coefficients* of their cars (Fig. 15–21). The drag coefficients of vehicles range from about 1.0 for large semi-trucks to 0.4 for minivans, and to 0.3 for passenger cars. In general, the more blunt the vehicle, the higher the drag coefficient.
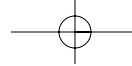
Installing a fairing reduces the drag coefficient of tractor-trailer rigs by about 20 percent by making the frontal surface more streamlined. As a rule of thumb, the percentage of fuel savings due to reduced drag is about half the percentage of drag reduction.

From the drag point of view, the ideal shape of a *vehicle* is the basic *teardrop,* with a drag coefficient of about 0.1 for the turbulent flow case. But this shape needs to be modified to accommodate several necessary external components such as wheels, mirrors, axles, antennas, and so on. Also, the vehicle must be high enough for comfort and there must be a minimum clearance from the road. Further, a vehicle cannot be too long to fit in garages and parking spaces. Controlling the material and manufacturing costs requires minimizing or eliminating any "dead" volume that cannot be utilized. The result is a shape that resembles more of a "box" than a "teardrop," and this was the shape of early cars with a drag coefficient of 0.8 in the 1920s. This wasn't a problem in those days since the velocities were low and drag was not a major design consideration.

The average drag coefficients of cars dropped to about 0.70 in the 1940s, to 0.55 in the 1970s, to 0.45 in the 1980s, and to 0.30 in the 1990s as a result of improved manufacturing techniques for metal forming and paying more attention to the shape of the car and streamlining. The drag coefficient for well-built racing cars is about 0.2, but this is achieved after making the comfort of drivers a secondary consideration. Noting that the theoretical lower limit of C_D is about 0.1 and the value for racing cars is 0.2, it appears that there is only little room for further improvement in the drag coefficient of passenger cars from the current value of 0.3. For trucks and buses, the drag coefficient can be reduced further by optimizing the front and rear contours (by rounding, for example) to the extent it is practical while keeping the overall length of the vehicle the same.

When traveling as a group, a sneaky way of reducing drag is **drafting,** a phenomenon well known by bicycle riders and car racers. It involves approaching a moving body from behind and *being drafted* into the low-pressure region in the rear of the body. The drag coefficient of a racing bicyclist, for example, can be reduced from 0.9 to 0.5 by drafting, as shown in Table 15–2 (Fig. 15–22).

We also can help reduce the overall drag of a vehicle and thus fuel consumption by being more conscientious drivers. For example, drag force is proportional to the square of velocity. Therefore, driving over the speed limit on the highways not only increases the chances of getting speeding tickets, but it also increases the amount of fuel consumption per mile. Therefore, driving at moderate speeds is safe and economical. Also, anything that extends from the car, even an arm, increases the drag coefficient. Driving with the windows rolled down also increases the drag and fuel consumption. At highway speeds,

FIGURE 15–21
Streamlines around an aerodynamically designed modern car closely resemble the streamlines around the car in the ideal potential flow (assumes negligible friction), resulting in a low drag coefficient. (from G. M. Homsy, et at.)

$C_D = 0.5$ $C_D = 0.9$

High pressure   Low pressure

FIGURE 15–22
The drag coefficients of bodies following other moving bodies closely can be reduced considerably due to drafting (i.e., falling into the vacuum created by the body in front).
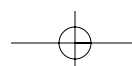
a driver can save fuel in hot weather by running the air conditioner instead of driving with the windows rolled down. Usually the turbulence and additional drag generated by open windows consume more fuel than does the air conditioner.

Superposition

The shapes of many bodies encountered in practice are not simple. But such bodies can be treated conveniently in drag force calculations by considering them to be composed of two or more simple bodies. A satellite dish mounted on a roof with a cylindrical bar, for example, can be considered to be a combination of a hemispherical body and a cylinder. Then the drag coefficient of the body can be determined approximately by using **superposition.** Such a simplistic approach does not account for the effects of components on each other, and thus the results obtained should be interpreted accordingly.

Flat mirror
95 km/h
$D = 13$ cm

Rounded
mirror
95 km/h
$D = 13$ cm
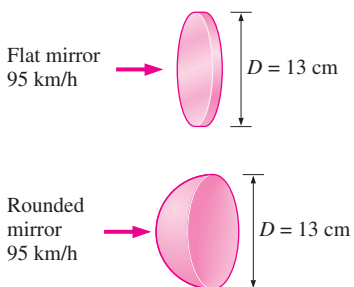
FIGURE 15–23
Schematic for Example 15–2.

EXAMPLE 15–2   **Effect of Mirror Design on the Fuel Consumption of a Car**

As part of the continuing efforts to reduce the drag coefficient and thus to improve the fuel efficiency of cars, the design of side rearview mirrors has changed drastically from a simple circular plate to a streamlined shape. Determine the amount of fuel and money saved per year as a result of replacing a 13-cm-diameter flat mirror by one with a hemispherical back (Fig. 15–23). Assume the car is driven 24,000 km a year at an average speed of 95 km/h. Take the density and price of gasoline to be 0.8 kg/L and $0.60/L, respectively; the heating value of gasoline to be 44,000 kJ/kg; and the overall efficiency of the engine to be 30 percent.

SOLUTION   The flat mirror of a car is replaced by one with a hemispherical back. The amount of fuel and money saved per year as a result are to be determined.

Assumptions   **1** The car is driven 24,000 km a year at an average speed of 95 km/h. **2** The effect of the car body on the flow around the mirror is negligible (no interference). **3** The average density of air is 1.20 kg/m³.

Properties   The densities of air and gasoline are taken to be 1.20 kg/m³ and 800 kg/m³, respectively. The heating value of gasoline is given to be 44,000 kJ/kg. The drag coefficients C_D are 1.1 for a circular disk and 0.40 for a hemispherical body (Table 15–2).

Analysis   The drag force acting on a body is determined from

$$F_D = C_D A \frac{\rho \mathcal{V}^2}{2}$$

where A is the frontal area of the body, which is $A = \pi D^2/4$ for both the flat and rounded mirrors. The drag force acting on the flat mirror is

$$F_D = 1.1 \frac{\pi(0.13 \text{ m})^2}{4} \frac{(1.20 \text{ kg/m}^3)(95 \text{ km/h})^2}{2} \left(\frac{1 \text{ m/s}}{3.6 \text{ km/h}}\right)^2 \left(\frac{1 \text{ N}}{1 \text{ kg} \cdot \text{m/s}^2}\right) = 6.10 \text{ N}$$

Noting that work is force times distance, the amount of work done to overcome this drag force and the required energy input for a distance of 24,000 km are

$$W_{drag} = F_D \times L = (6.10 \text{ N})(24{,}000 \text{ km/year}) = 146{,}400 \text{ kJ/year}$$

$$E_{in} = \frac{W_{drag}}{\eta_{car}} = \frac{146{,}400 \text{ kJ/year}}{0.3} = 488{,}000 \text{ kJ/year}$$

Then the amount and costs of the fuel that supplies this much energy are

$$\text{Amount of fuel} = \frac{m_{fuel}}{\rho_{fuel}} = \frac{E_{in}/HV}{\rho_{fuel}} = \frac{(488{,}000 \text{ kJ/year})/(44{,}000 \text{ kJ/kg})}{0.8 \text{ kg/L}} = 13.9 \text{ L/year}$$

$$\text{Cost} = (\text{Amount of fuel})(\text{Unit cost}) = (13.9 \text{ L/year})(\$0.60/\text{L}) = \$8.32/\text{year}$$

That is, the car uses 13.9 L of gasoline at a cost of \$8.32 per year to overcome the drag generated by a flat mirror extending out from the side of a car.

The drag force and the work done to overcome it are directly proportional to the drag coefficient. Then the percent reduction in the fuel consumption due to replacing the mirror is equal to the percent reduction in the drag coefficient:

$$\text{Reduction ratio} = \frac{C_{D,\,flat} - C_{D,\,hemisp}}{C_{D,\,flat}} = \frac{1.1 - 0.4}{1.1} = 0.636$$

$$\text{Fuel reduction} = (\text{Reduction ratio})(\text{Amount of fuel})$$
$$= 0.636(13.9 \text{ L/year}) = \textbf{8.84 L/year}$$

$$\text{Cost reduction} = (\text{Reduction ratio})(\text{Cost}) = 0.636(\$8.32/\text{year}) = \textbf{\$5.29/year}$$

Therefore, replacing a flat mirror by a hemispherical one reduces the fuel consumption due to mirror drag by 63.6 percent.

Discussion   Note from this example that significant reductions in drag and fuel consumption can be achieved by streamlining the shape of various components and the entire car. So it is no surprise that the sharp corners are replaced in late model cars by rounded contours. This also explains why large airplanes retract their wheels after takeoff and small airplanes use contoured fairings around their wheels.

Example 15–2 is indicative of the tremendous amount of effort put in recent years into redesigning various parts of cars such as the window moldings, the door handles, the windshield, and the front and rear ends in order to reduce aerodynamic drag. For a car moving on a level road at constant speed, the power developed by the engine is used to overcome rolling resistance, friction between moving components, aerodynamic drag, and driving the auxiliary equipment. The aerodynamic drag is negligible at low speeds, but becomes significant at speeds above about 30 mph. Reduction of the frontal area of the cars (to the dislike of tall drivers) has also contributed greatly to the reduction of drag and fuel consumption.

15–5 ▪ PARALLEL FLOW OVER FLAT PLATES

Consider the flow of a fluid over a *flat plate,* as shown in Fig. 15–24. Surfaces that are slightly contoured such as turbine blades can also be approximated as
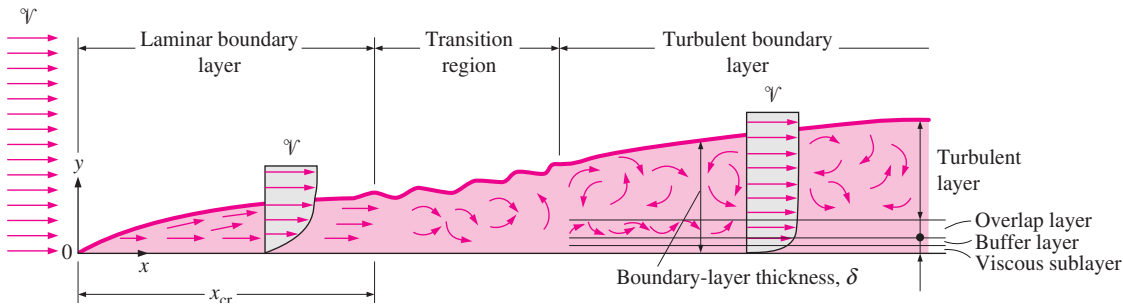
FIGURE 15–24
The development of the boundary layer for flow over a flat plate, and the different flow regimes.
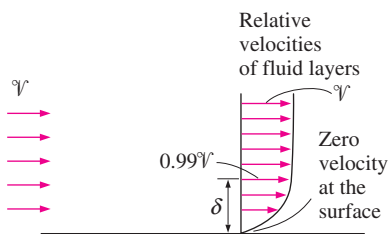
FIGURE 15–25
The development of a boundary layer on a surface is due to the no-slip condition.

FIGURE 15–26
For parallel flow over a flat plate, the pressure drag is zero, and thus the drag coefficient is equal to the friction coefficient and the drag force is equal to the friction force.

flat plates with reasonable accuracy. The x-coordinate is measured along the plate surface from the *leading edge* of the plate in the direction of the flow, and y is measured from the surface in the normal direction. The fluid approaches the plate in the x-direction with a uniform velocity $\mathcal{V}$, which is equivalent to the velocity over the plate away from the surface.

For the sake of discussion, we can consider the fluid to consist of adjacent layers piled on top of each other. The velocity of the particles in the first fluid layer adjacent to the plate becomes zero because of the no-slip condition. This motionless layer slows down the particles of the neighboring fluid layer as a result of friction between the particles of these two adjoining fluid layers at different velocities. This fluid layer then slows down the molecules of the next layer, and so on. Thus, the presence of the plate is felt up to some normal distance δ from the plate beyond which the free-stream velocity remains unchanged. As a result, the x-component of the fluid velocity, u, will vary from 0 at $y = 0$ to nearly $\mathcal{V}$ at $y = \delta$ (Fig. 15–25).

The region of the flow above the plate bounded by δ in which the effects of the viscous shearing forces caused by fluid viscosity are felt is called the **velocity boundary layer.** The *boundary layer thickness*, δ, is typically defined as the distance y from the surface at which $u = 0.99\,\mathcal{V}$.

The hypothetical line of $u = 0.99\,\mathcal{V}$ divides the flow over a plate into two regions: the **boundary layer region,** in which the viscous effects and the velocity changes are significant, and the **irrotational flow region,** in which the frictional effects are negligible and the velocity remains essentially constant.

For parallel flow over a flat plate, the pressure drag is zero, and thus the drag coefficient is equal to the *friction drag coefficient,* or simply the *friction coefficient* (Fig. 15–26). That is,

Flat plate: $$C_D = C_{D, \text{friction}} = C_f \qquad \text{(15–13)}$$

Once the average friction coefficient C_f is available, the drag (or friction) force over the surface can be determined from

Friction force on a flat plate: $$F_D = F_f = \tfrac{1}{2}\,C_f A \mathcal{V}^2 \qquad \text{(15–14)}$$

where A is the surface area of the plate exposed to fluid flow. When both sides of a thin plate are subjected to flow, A becomes the total area of the top and bottom surfaces. Note that the friction coefficient, in general, varies with location along the surface.

Typical mean velocity profiles in laminar and turbulent flow are also given in Fig. 15–24. Note that the velocity profile in turbulent flow is much fuller than that in laminar flow, with a sharp drop near the surface. The turbulent boundary layer can be considered to consist of four regions, characterized by the distance from the wall. The very thin layer next to the wall where viscous effects are dominant is the **viscous** sublayer. The velocity profile in this layer is very nearly *linear*, and the flow is streamlined. Next to the viscous sublayer is the **buffer layer,** in which turbulent effects are becoming significant, but the flow is still dominated by viscous effects. Above the buffer layer is the **over-lap layer,** in which the turbulent effects are much more significant, but still not dominant. Above that is the **turbulent layer** in which turbulent effects dominate over viscous effects. Note that the turbulent boundary layer profile on a flat plate closely resembles the boundary layer profile in fully developed turbulent pipe flow.

The transition from laminar to turbulent flow depends on the *surface geometry, surface roughness, upstream velocity, surface temperature,* and the *type of fluid,* among other things, and is best characterized by the Reynolds number. The Reynolds number at a distance x from the leading edge of a flat plate is expressed as

$$\text{Re}_x = \frac{\rho \mathcal{V} x}{\mu} = \frac{\mathcal{V} x}{\upsilon} \qquad \textbf{(15–15)}$$

where $\mathcal{V}$ is the upstream velocity and x is the characteristic length of the geometry, which, for a flat plate, is the length of the plate in the flow direction. Note that unlike pipe flow, the Reynolds number varies for a flat plate along the flow, reaching $\text{Re}_L = \mathcal{V} L / \upsilon$ at the end of the plate. For any point on a flat plate, the characteristic length is the distance x of the point from the leading edge in the flow direction.

For flow over a *flat plate,* transition from laminar to turbulent begins at about $\text{Re} \approx 1 \times 10^5$, but does not become fully turbulent before the Reynolds number reaches much higher values. A generally accepted value for the critical Reynolds number is

$$\text{Re}_{x,\,cr} = \frac{\rho \mathcal{V} x_{cr}}{\mu} = 5 \times 10^5$$

This generally accepted value of the critical Reynolds number for a flat plate may vary somewhat from about 10^5 to 3×10^6 depending on the surface roughness, the turbulence level, and the variation of pressure along the surface.

Friction Coefficient

The friction coefficient for a flat plate can be determined theoretically by solving the conservation of mass and momentum equations approximately or numerically. It can also be determined experimentally and expressed by empirical correlations.

The local friction coefficient *varies* along the surface of the flat plate as a result of the changes in the velocity boundary layer in the flow direction. We are usually interested in the drag force on the *entire* surface, which can be determined using the *average* friction coefficient. But sometimes we are also interested in the drag force at a certain location, and in such cases, we need to know
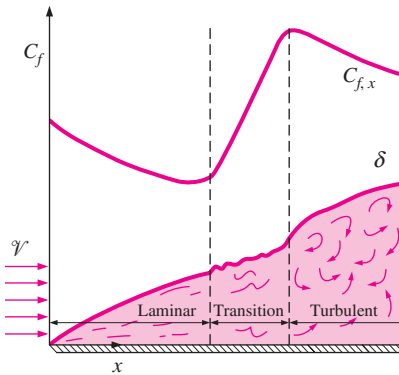
the *local* value of the friction coefficient. With this in mind, below we present correlations for both local (identified with the subscript x) and average friction coefficients over a flat plate for *laminar, turbulent,* and *combined laminar and turbulent* flow conditions. Once the local values are available, the *average* friction coefficient for the entire plate can be determined by integration from

$$C_f = \frac{1}{L}\int_0^L C_{f,x}\, dx \tag{15–16}$$

Based on analysis, the boundary layer thickness and the local friction coefficient at location x for laminar flow over a flat plate were determined to be

Laminar: $\qquad \delta = \dfrac{4.91x}{\mathrm{Re}_x^{1/2}}$ and $C_{f,x} = \dfrac{0.664}{\mathrm{Re}_x^{1/2}}, \quad \mathrm{Re}_x < 5 \times 10^5 \tag{15–17}$

The corresponding relations for turbulent flow are

Turbulent: $\qquad \delta = \dfrac{0.38x}{\mathrm{Re}_x^{1/5}}$ and $C_{f,x} = \dfrac{0.059}{\mathrm{Re}_x^{1/5}}, \quad 5 \times 10^5 \leq \mathrm{Re}_x \leq 10^7 \tag{15–18}$

where x is the distance from the leading edge of the plate and $\mathrm{Re}_x = \mathcal{V}x/\upsilon$ is the Reynolds number at location x. Note that $C_{f,x}$ is proportional to $1/\mathrm{Re}_x^{1/2}$ and thus to $x^{-1/2}$ for laminar flow. Therefore, $C_{f,x}$ is supposedly *infinite* at the leading edge ($x = 0$) and decreases by a factor of $x^{-1/2}$ in the flow direction. The variation of the boundary layer thickness δ and the friction coefficient $C_{f,x}$ along a flat plate is shown in Fig. 15–27. The local friction coefficients are higher in turbulent flow than they are in laminar flow because of the intense mixing that occurs in the turbulent boundary layer. Note that $C_{f,x}$ reaches its highest values when the flow becomes fully turbulent, and then decreases by a factor of $x^{-1/5}$ in the flow direction, as shown in the figure.

The *average* friction coefficient over the entire plate is determined by substituting the preceding relations into Eq. 15–16 and performing the integrations (Fig. 15–28). We get

Laminar: $\qquad C_f = \dfrac{1.328}{\mathrm{Re}_L^{1/2}} \qquad \mathrm{Re}_L < 5 \times 10^5 \tag{15–19}$

Turbulent: $\qquad C_f = \dfrac{0.074}{\mathrm{Re}_L^{1/5}}, \qquad 5 \times 10^5 \leq \mathrm{Re}_L \leq 10^7 \tag{15–20}$

The first of these relations gives the average friction coefficient for the entire plate when the flow is *laminar* over the *entire* plate. The second relation gives the average friction coefficient for the entire plate only when the flow is *turbulent* over the *entire* plate, or when the laminar flow region of the plate is negligibly small relative to the turbulent flow region (that is, $x_{cr} \ll L$ where the length of the plate x_{cr} over which the flow is laminar can be determined from $\mathrm{Re}_{cr} = 5 \times 10^5 = \mathcal{V}x_{cr}/\upsilon$).

In some cases, a flat plate is sufficiently long for the flow to become turbulent, but not long enough to disregard the laminar flow region. In such cases, the *average* friction coefficient over the entire plate is determined by performing the integration in Eq. 15–16 over two parts: the laminar region $0 \leq x \leq x_{cr}$ and the turbulent region $x_{cr} < x \leq L$ as

FIGURE 15–27
The variation of the local friction coefficient for flow over a flat plate. Note that the vertical scale of the boundary layer is greatly exaggerated in this sketch.

FIGURE 15–28
The average friction coefficient over a surface is determined by integrating the local friction coefficient over the entire surface. The values shown here are for a laminar flat plate boundary layer.

$$C_f = \frac{1}{L}\left(\int_0^{x_{cr}} C_{f,x,\text{laminar}}\, dx + \int_{x_{cr}}^{L} C_{f,x,\text{turbulent}}\, dx\right) \qquad \textbf{(15–21)}$$

Note that we included the transition region with the turbulent region. Again taking the critical Reynolds number to be $\text{Re}_{cr} = 5 \times 10^5$ and performing these integrations after substituting the indicated expressions, the *average* friction coefficient over the *entire* plate is determined to be

$$C_f = \frac{0.074}{\text{Re}_L^{1/5}} - \frac{1742}{\text{Re}_L}, \qquad 5 \times 10^5 \leq \text{Re}_L \leq 10^7 \qquad \textbf{(15–22)}$$

The constants in this relation will be different for different critical Reynolds numbers. Also, the surfaces are assumed to be *smooth*, and the free stream to be of very low turbulence intensity. For laminar flow, the friction coefficient depends on only the Reynolds number, and the surface roughness has no effect. For turbulent flow, however, surface roughness causes the friction coefficient to increase several fold, to the point that in fully turbulent regime the friction coefficient is a function of surface roughness alone, and independent of Reynolds number (Fig. 15–29). This is analogous to flow in pipes.

A curve fit of experimental data for the average friction coefficient in this regime is given by Schlichting as

Rough surface, turbulent: $\qquad C_f = \left(1.89 - 1.62 \log \frac{\varepsilon}{L}\right)^{-2.5} \qquad \textbf{(15–23)}$

where ε is the surface roughness and L is the length of the plate in the flow direction. In the absence of a better relation, the relation above can be used for turbulent flow on rough surfaces for $\text{Re} > 10^6$, especially when $\varepsilon/L > 10^{-4}$.

Friction coefficients C_f for parallel flow over smooth and rough flat plates are plotted in Fig. 15–30 for both laminar and turbulent flows. Note that C_f increases several fold with roughness in turbulent flow. Also note that C_f is

Relative roughness, ε/L	Friction coefficient C_f
0.0*	0.0029
1×10^{-5}	0.0032
1×10^{-4}	0.0049
1×10^{-3}	0.0084

*Smooth surface for $\text{Re} = 10^7$. Others calculated from Eq. 15–23.

FIGURE 15–29
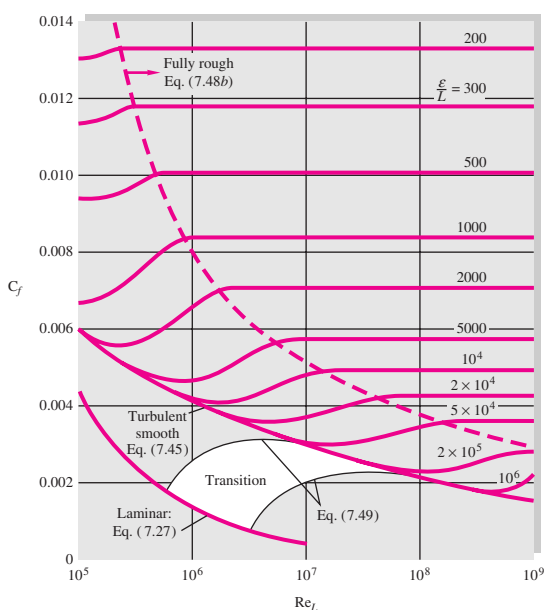For turbulent flow, surface roughness may cause the friction coefficient to increase severalfold.

FIGURE 15–30
Friction coefficient for parallel flow over smooth and rough flat plates. (from White)
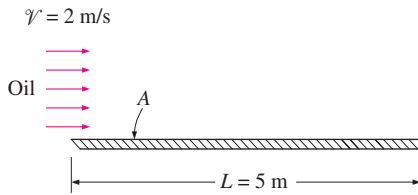
independent of Reynolds number in the fully rough region. This chart is the flat-plate analog of the Moody chart for pipe flows.

$\mathscr{V} = 2$ m/s

Oil

A

$L = 5$ m

FIGURE 15–31
Schematic for Example 15–3.

EXAMPLE 15–3   **Flow of Hot Oil over a Flat Plate**

Engine oil at 40°C flows over a 5-m-long flat plate with a free stream velocity of 2 m/s (Fig. 15–31). Determine the drag force acting on the plate per unit width.

SOLUTION   Engine oil flows over a flat plate. The drag force per unit width of the plate is to be determined.

Assumptions   **1** The flow is steady and incompressible. **2** The critical Reynolds number is $\text{Re}_{cr} = 5 \times 10^5$.

Properties   The density and kinematic viscosity of engine oil at 40°C are $\rho = 876$ kg/m^3 and $v = 2.485 \times 10^{-4}$ m^2/s (Table A–19).

Analysis   Noting that $L = 5$ m, the Reynolds number at the end of the plate is

$$\text{Re}_L = \frac{\mathscr{V}L}{v} = \frac{(2 \text{ m/s})(5 \text{ m})}{2.485 \times 10^{-4} \text{ m}^2/\text{s}} = 4.024 \times 10^4$$

which is less than the critical Reynolds number. Thus we have *laminar flow* over the entire plate, and the average friction coefficient is

$$C_f = 1.328 \text{ Re}_L^{-0.5} = 1.328 \times (4.024 \times 10^4)^{-0.5} = 0.00662$$

Noting that the pressure drag is zero and thus $C_D = C_f$ for parallel flow over a flat plate, the drag force acting on the plate per unit width becomes

$$F_D = C_f A \frac{\rho \mathscr{V}^2}{2} = 0.00662 \times (5 \times 1 \text{ m}^2) \frac{(876 \text{ kg/m}^3)(2 \text{ m/s})^2}{2} \left(\frac{1 \text{ N}}{1 \text{ kg} \cdot \text{m/s}^2}\right) = \textbf{58.0 N}$$

The total drag force acting on the entire plate can be determined by multiplying the value just obtained by the width of the plate.

Discussion   The force per unit width corresponds to the weight of a mass of about 6 kg. Therefore, a person who applies an equal and opposite force to the plate to keep it from moving will feel like he or she is using as much force as is necessary to hold a 6-kg mass from dropping.

15–6 ▪ FLOW ACROSS CYLINDERS AND SPHERES

Flow across cylinders and spheres is frequently encountered in practice. For example, the tubes in a shell-and-tube heat exchanger involve both *internal flow* through the tubes and *external flow* over the tubes, and both flows must be considered in the analysis of the heat exchanger. Also, many sports such as soccer, tennis, and golf involve flow over spherical balls.

The characteristic length for a circular cylinder or sphere is taken to be the *external diameter D*. Thus, the Reynolds number is defined as $\text{Re} = \mathscr{V}D/v$ where $\mathscr{V}$ is the uniform velocity of the fluid as it approaches the cylinder or sphere. The critical Reynolds number for flow across a circular cylinder or sphere is about $\text{Re}_{cr} \approx 2 \times 10^5$. That is, the boundary layer remains laminar for about $\text{Re} \lesssim 2 \times 10^5$ and becomes turbulent for $\text{Re} \gtrsim 2 \times 10^5$.
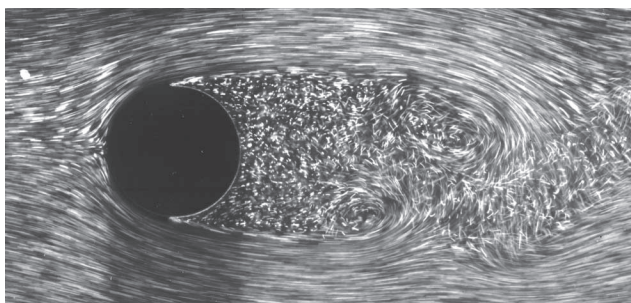
FIGURE 15–32
Laminar boundary layer separation with a turbulent wake; flow over a circular cylinder at Re = 2000. (Courtesy ONERA, photograph by Werle).
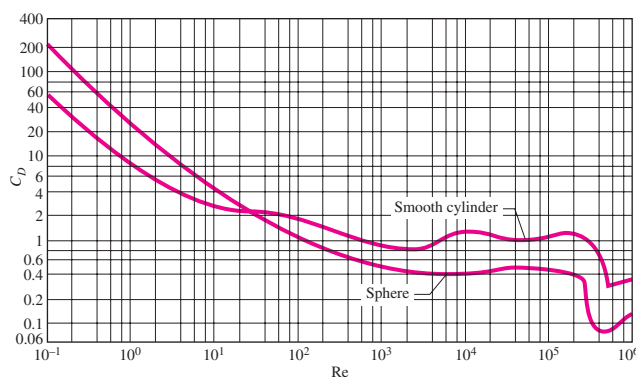
FIGURE 15–33
Average drag coefficient for cross-flow over a smooth circular cylinder and a smooth sphere. (from Schlichting. Used with permission.)

Cross-flow over a cylinder exhibits complex flow patterns, as shown in Fig. 15–32. The fluid approaching the cylinder branches out and encircles the cylinder, forming a boundary layer that wraps around the cylinder. The fluid particles on the midplane strike the cylinder at the stagnation point, bringing the fluid to a complete stop and thus raising the pressure at that point. The pressure decreases in the flow direction while the fluid velocity increases.

At very low upstream velocities (Re ≲ 1), the fluid completely wraps around the cylinder and the two arms of the fluid meet on the rear side of the cylinder in an orderly manner. Thus, the fluid follows the curvature of the cylinder. At higher velocities, the fluid still hugs the cylinder on the frontal side, but it is too fast to remain attached to the surface as it approaches the top of the cylinder. As a result, the boundary layer detaches from the surface, forming a separation region behind the cylinder. Flow in the wake region is characterized by periodic vortex formation and pressures much lower than the stagnation point pressure.

The nature of the flow across a cylinder or sphere strongly affects the total drag coefficient C_D. Both the *friction drag* and the *pressure drag* can be significant. The high pressure in the vicinity of the stagnation point and the low pressure on the opposite side in the wake produce a net force on the body in the direction of flow. The drag force is primarily due to friction drag at low Reynolds numbers (Re < 10) and to pressure drag at high Reynolds numbers (Re > 5000). Both effects are significant at intermediate Reynolds numbers.

The average drag coefficients C_D for cross-flow over a smooth single circular cylinder and a sphere are given in Fig. 15–33. The curves exhibit different behaviors in different ranges of Reynolds numbers:

- For Re $\lesssim$ 1, we have creeping flow, and the drag coefficient decreases with increasing Reynolds number. For a sphere, it is $C_D = 24/\text{Re}$. There is no flow separation in this regime.

- At about Re $= 10$, separation starts occurring on the rear of the body with vortex shedding starting at about Re ≈ 90. The region of separation increases with increasing Reynolds number up to about Re $= 10^3$. At this point, the drag is mostly (about 95 percent) due to pressure drag. The drag coefficient continues to decrease with increasing Reynolds number in this range of $10 < \text{Re} < 10^3$. (A decrease in the drag coefficient does not necessarily indicate a decrease in drag. The drag force is proportional to the square of the velocity, and the increase in velocity at higher Reynolds numbers usually more than offsets the decrease in the drag coefficient.)

- In the moderate range of $10^3 < \text{Re} < 10^5$, the drag coefficient remains relatively constant. This behavior is characteristic of blunt bodies. The flow in the boundary layer is laminar in this range, but the flow in the separated region past the cylinder or sphere is highly turbulent with a wide turbulent wake.

- There is a sudden drop in the drag coefficient somewhere in the range of $10^5 < \text{Re} < 10^6$ (usually, at about 2×10^5). This large reduction in C_D is due to the flow in the boundary layer becoming *turbulent,* which moves the separation point further on the rear of the body, reducing the size of the wake and thus the magnitude of the pressure drag. This is in contrast to streamlined bodies, which experience an increase in the drag coefficient (mostly due to friction drag) when the boundary layer becomes turbulent.
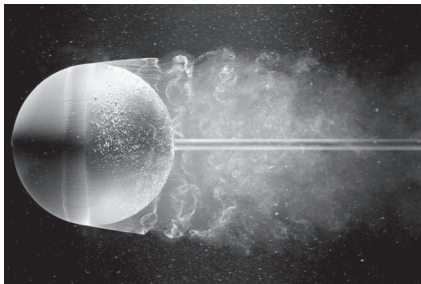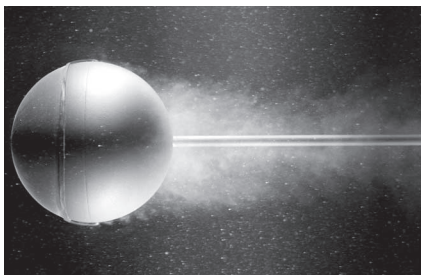
Flow separation occurs at about $\theta \approx 80°$ (measured from the stagnation point) when the boundary layer is *laminar* and at about $\theta \approx 140°$ when it is *turbulent* (Fig. 15–34). The delay of separation in turbulent flow is caused by the rapid fluctuations of the fluid in the transverse direction, which enables the turbulent boundary layer to travel farther along the surface before separation occurs, resulting in a narrower wake and a smaller pressure drag. In the range of Reynolds numbers where the flow changes from laminar to turbulent, even the drag force F_D decreases as the velocity (and thus Reynolds number) increases. This results in a sudden decrease in drag of a flying body (sometimes called the *drag crisis*) and instabilities in flight.

Effect of Surface Roughness

We mentioned earlier that *surface roughness,* in general, increases the drag coefficient in turbulent flow. This is especially the case for streamlined bodies. For blunt bodies such as a circular cylinder or sphere, however, an increase in the surface roughness may actually *decrease* the drag coefficient, as shown in Fig. 15–35 for a sphere. This is done by tripping the boundary layer into turbulence at a lower Reynolds number, and thus causing the fluid to close in behind the body, narrowing the wake and reducing pressure drag considerably. This results in a much smaller drag coefficient and thus drag force for a rough-surfaced cylinder or sphere in a certain range of Reynolds number compared to a smooth one of identical size at the same velocity. At Re $= 10^5$, for example, $C_D = 0.1$ for a rough sphere with $\varepsilon/D = 0.0015$, whereas $C_D = 0.5$ for a smooth one. Therefore, the drag coefficient in this case is reduced by a factor of 5 by simply roughening the surface. Note, however, that at Re $= 10^6$, $C_D = 0.4$ for the rough
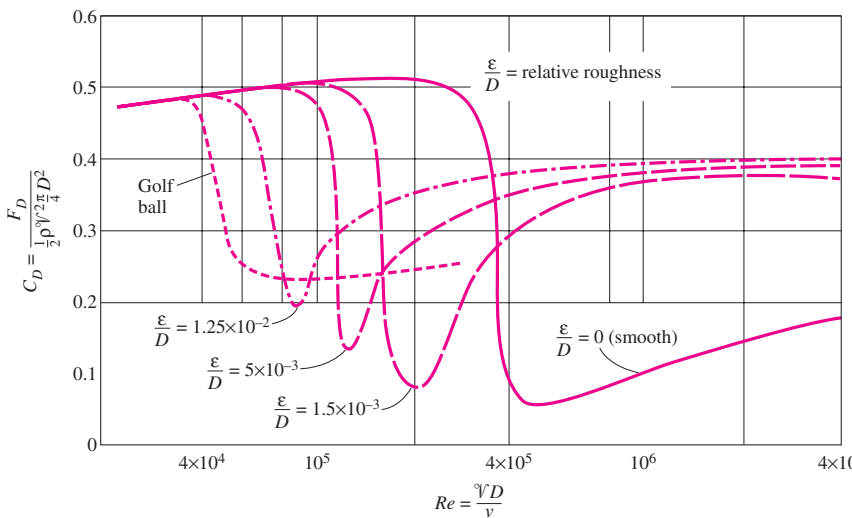
(a)

(b)

FIGURE 15-34
Flow visualization of flow over (*a*) a smooth sphere at Re $= 15,000$, and (*b*) a sphere at Re $= 30,000$ with a trip wire. The delay of boundary layer separation is clearly seen by comparing the two photographs. (Courtesy, ONERA, photograph by Werle).

FIGURE 15–35
The effect of surface roughness on the drag coefficient of a sphere (from Blevins, Ref. 5).

sphere while $C_D = 0.1$ for the smooth one. Obviously, roughening the sphere in this case will increase the drag by a factor of 4 (Fig. 15–36).

The preceding discussion shows that roughening the surface can be used to great advantage in reducing drag, but it can also backfire on us if we are not careful—specifically, if we do not operate in the right range of Reynolds number. With this consideration, golf balls are intentionally roughened to induce *turbulence* at a lower Reynolds number to take advantage of the sharp *drop* in the drag coefficient at the onset of turbulence in the boundary layer (the typical velocity range of golf balls is 15 to 150 m/s, and the Reynolds number is less than 4×10^5). The critical Reynolds number of dimpled golf balls is about 4×10^4. The occurrence of turbulent flow at this Reynolds number reduces the drag coefficient of a golf ball by half, as shown in Fig. 15–35. For a given hit, this means a longer distance for the ball. Experienced golfers also give the ball a spin during the hit, which helps the rough ball develop a lift and thus travel higher and farther. A similar argument can be given for a tennis ball. For a table tennis ball, however, the distances are very short, and the balls never reach the speeds in the turbulent range. Therefore, the surfaces of table tennis balls are made smooth.

Once the drag coefficient is available, the drag force acting on a body in cross-flow can be determined from Eq. 15–1 where A is the *frontal area* ($A = LD$ for a cylinder of length L and $A = \pi D^2/4$ for a sphere). It should be kept in mind that free-stream turbulence and disturbances by other bodies in flow (such as flow over tube bundles) may affect the drag coefficients significantly.

| | C_D | |
Re	Smooth surface	Rough surface, $\varepsilon/L = 0.0015$
10^5	0.5	0.1
10^6	0.1	0.4

FIGURE 15–36
Surface roughness may increase or decrease the drag coefficient of a spherical object, depending on the value of the Reynolds number.

EXAMPLE 15–4   **Drag Force Acting on a Pipe in a River**

A 2.2-cm-outer-diameter pipe is to cross a river at a 30-m-wide section while being completely immersed in water (Fig. 15–37). The average flow velocity of water is 4 m/s and the water temperature is 15°C. Determine the drag force exerted on the pipe by the river.

SOLUTION   A pipe is crossing a river. The drag force that acts on the pipe is to be determined.
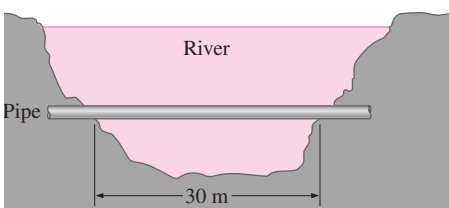
FIGURE 15–37
Schematic for Example 15–4.

Assumptions **1** The outer surface of the pipe is smooth so that Fig. 15–30 can be used to determine the drag coefficient. **2** Water flow in the river is steady. **3** The direction of water flow is normal to the pipe. **4** Turbulence in river flow is not considered.

Properties The density and dynamic viscosity of water at 15°C are $\rho = 999.1$ kg/m^3 and $\mu = 1.138 \times 10^{-3}$ kg/m · s (Table A–15).

Analysis Noting that $D = 0.022$ m, the Reynolds number is

$$\text{Re} = \frac{\mathcal{V}D}{\upsilon} = \frac{\rho \mathcal{V}D}{\mu} = \frac{(999.1 \text{ kg/m}^3)(4 \text{ m/s})(0.022 \text{ m})}{1.138 \times 10^{-3} \text{ kg/m} \cdot \text{s}} = 7.73 \times 10^4$$

The drag coefficient corresponding to this value is, from Fig. 15–33, $C_D = 1.0$. Also, the frontal area for flow past a cylinder is $A = LD$. Then the drag force acting on the pipe becomes

$$F_D = C_D A \frac{\rho \mathcal{V}^2}{2} = 1.0(30 \times 0.022 \text{ m}^2) \frac{(999.1 \text{ kg/m}^3)(4 \text{ m/s})^2}{2} \left(\frac{1 \text{ N}}{1 \text{ kg} \cdot \text{m/s}^2} \right)$$

$$= \textbf{5275 N}$$

Discussion Note that this force is equivalent to the weight of a mass over 500 kg. Therefore, the drag force the river exerts on the pipe is equivalent to hanging a total of over 500 kg in mass on the pipe supported at its ends 30 m apart. The necessary precautions should be taken if the pipe cannot support this force. If the river were to flow at a faster speed, turbulent fluctuations in the river might be significant, and the drag force would be even larger. *Unsteady* forces on the pipe might then be significant.

15–7 ▪ LIFT

Lift was defined earlier as the component of the net force (due to viscous and pressure forces) that is perpendicular to the flow direction, and the lift coefficient was expressed as

$$C_L = \frac{F_L}{\frac{1}{2}\rho \mathcal{V}^2 A} \tag{15–6}$$

where A in this case is normally the *planform area,* which is the area that would be seen by a person looking at the body from above in a direction normal to the body, and $\mathcal{V}$ is the upstream velocity of the fluid (or, equivalently, the velocity of a flying body in a quiescent fluid). For an airfoil of width (or span) b and chord length c (the length between the leading and trailing edges),
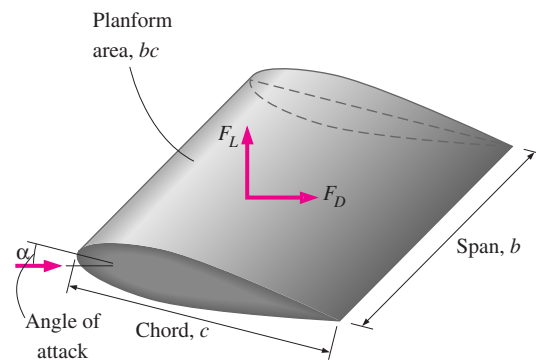
FIGURE 15–38
Definition of various terms
associated with an airfoil.

the planform area is $A = bc$. The distance between the two ends of a wing or airfoil is called the **wingspan** or just **span.** For an aircraft, the wingspan is taken to be the total distance between the tips of the two wings, which includes the width of the fuselage between the wings (Fig. 15–38). The average lift per unit planform area F_L/A is called the **wing loading,** which is simply the ratio of the weight of the aircraft to the planform area of the wings (since lift equals the weight during flying at constant altitude).

Airplane flights is based on lift, and thus developing a better understanding of lift as well as improving the lift characteristics of bodies have been the focus of numerous studies. Our emphasis in this sec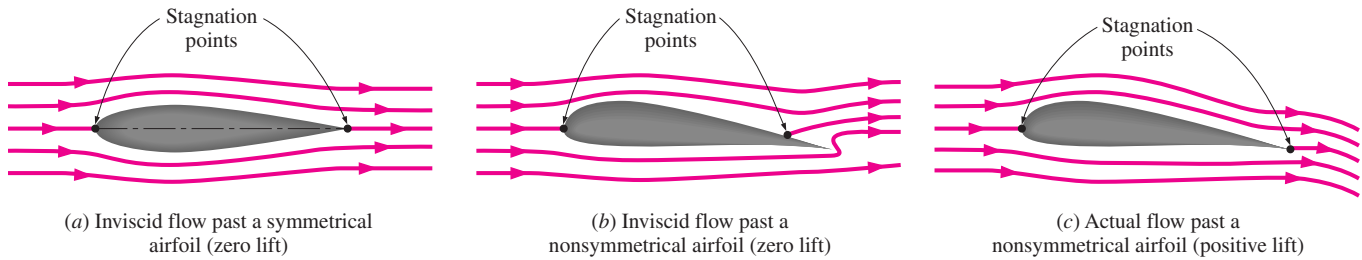tion is on devices such as *airfoils* that are specifically designed to generate lift while keeping the drag at a minimum. But it should be kept in mind that some devices such as the *spoilers* and *inverted airfoils* on racing cars are designed for the opposite purpose of avoiding lift or even generating negative lift to improve traction and control (some early cars actually "took off" at high speeds as a result of the lift produced, which alerted the engineers to come up with ways to reduce lift in their design).

For devices that are intended to generate lift such as airfoils, the contribution of *viscous effects* to lift is usually negligible since the bodies are streamlined, and wall shear is parallel to the surfaces of such devices and thus nearly normal to the direction of lift (Fig. 15–39). Therefore, lift in practice can be taken to be due entirely to the pressure distribution on the surfaces of the body, and thus the shape of the body has the primary effect on lift. Then the primary consideration in the design of airfoils is minimizing the average pressure at the upper surface while maximizing it at the lower surface. The Bernoulli equation can be used as a guide in identifying the high- and low-pressure regions: *Pressure is low at locations where the flow velocity is high, and pressure is high at locations where the flow velocity is low.* Also, lift is practically independent of the surface roughness since roughness affects the wall shear, not the pressure. The contribution of shear to lift is usually significant for very small (lightweight) bodies that can fly at low velocities (and thus very low Reynolds numbers).

Noting that the contribution of viscous effects to lift is negligible, we should be able to determine the lift acting on an airfoil by simply integrating the pressure distribution around the airfoil. The pressure changes in the flow direction along the surface, but it remains essentially constant through the boundary layer in a direction normal to the surface. Therefore, it seems reasonable to
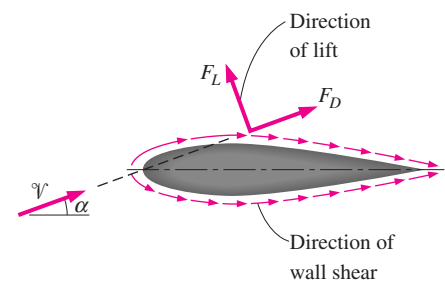
FIGURE 15–36
For airfoils, the contribution of viscous effects to lift is usually negligible since wall shear is parallel to the surfaces and thus nearly normal to the direction of lift.

Stagnation points
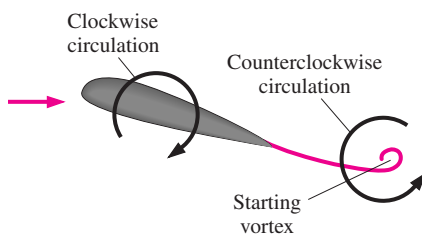
Stagnation points

Stagnation points

(*a*) Inviscid flow past a symmetrical airfoil (zero lift)

(*b*) Inviscid flow past a nonsymmetrical airfoil (zero lift)

(*c*) Actual flow past a nonsymmetrical airfoil (positive lift)

FIGURE 15–40
Inviscid (ideal) and actual flow past symmetrical and nonsymmetrical airfoils at zero angle of attack.

Clockwise circulation

Counterclockwise circulation

Starting vortex

FIGURE 15–41
Shortly after a sudden increase in angle of attack, a counterclockwise starting vortex is shed from the airfoil, while clockwise circulation appears around the airfoil, causing lift to be generated.

ignore the very thin boundary layer on the airfoil and calculate the pressure distribution around the airfoil from the relatively simple potential flow theory (zero vorticity, irrotational flow) for which net viscous forces are zero for flow past an airfoil.

The flow fields obtained from such calculations are sketched in Fig. 15–40 for both symmetrical and nonsymmetrical airfoils by ignoring the thin boundary layer. At zero angle of attack, the lift produced by the symmetrical airfoil is zero, as expected because of symmetry, and the stagnation points are at the leading and trailing edges. For the nonsymmetrical airfoil, the front stagnation point has moved down below the leading edge, and the rear stagnation point has moved up to the upper surface close to the trailing edge. To our surprise, the lift produced is calculated again to be zero—a clear contradiction of experimental observations and measurements. Obviously, the theory needs to be modified to bring it in line with the observed phenomenon.

The source of inconsistency is the rear stagnation point being at the upper surface instead of the trailing edge. This requires the lower side fluid to make a nearly U-turn and flow around the trailing edge toward the stagnation point while remaining attached to the surface, which is a physical impossibility since the observed phenomenon is the separation of flow at sharp turns (imagine a car attempting to make this turn at high speed). Therefore, if separation is to occur at a point (instead of over a region, which may occur at large angles of attack), it must occur at the trailing edge, and the stagnation point at the upper surface must move to the trailing edge. This way the two flow streams from the top and the bottom sides of the airfoil meet at the trailing edge, yielding a smooth flow downstream parallel to the chord line. Lift is generated because the flow velocity at the top surface is higher, and thus the pressure on that surface is lower due to the Bernoulli effect.

The potential flow theory and the observed phenomenon can be reconciled as follows: Flow starts out as predicted by theory, with no lift, but the lower fluid stream separates at the trailing edge when the velocity reaches a certain value. This forces the separated upper fluid stream to close in at the trailing edge, initiating clockwise circulation around the airfoil. This clockwise circulation increases the velocity of the upper stream while decreasing that of the lower stream, causing lift. A **starting vortex** of opposite sign (counterclockwise circulation) is then shed downstream (Fig. 15–41), and smooth streamlined flow is established over the airfoil. When the potential flow theory is modified by the addition of an appropriate amount of circulation to move the
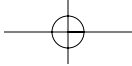
stagnation point down to the trailing edge, excellent agreement is obtained between theory and experiment for both the flow field and the lift.

It is desirable for airfoils to generate the most lift while producing the least drag. Therefore, a measure of performance for airfoils is the **lift-to-drag ratio,** which is equivalent to the ratio of the lift-to-drag coefficients C_L/C_D. This information is provided by either plotting C_L versus C_D for different values of the angle of attack (a lift-drag polar) or by plotting the ratio C_L/C_D versus the angle of attack. The latter is done for a particular airfoil design in Fig. 15–42. Note that the C_L/C_D ratio increases with the angle of attack until the airfoil stalls, and the value of the lift-to-drag can be in the order of 100.

One obvious way to change the lift and drag characteristics of an airfoil is to change the angle of attack. On an airplane, for example, the entire plane is pitched up to increase lift, since the wings are fixed relative to the fuselage. Another approach is to change the shape of the airfoil by the use of movable *leading edge* and *trailing edge flaps,* as is commonly done in modern large aircraft (Fig. 15–43). The flaps are used to alter the shape of the wings during takeoff and landing to maximize lift and to enable the aircraft to land or take off at low speeds. The increase in drag during this takeoff and landing is not much of a concern because of the relatively short time periods involved. Once at cruising altitude, the flaps are retracted, and the wing is returned to its "normal" shape with minimal drag coefficient and adequate lift coefficient to minimize fuel consumption while cruising at a constant altitude. Note that even a small lift coefficient can generate a large lift force during normal operation because of the large cruising velocities of aircraft and the proportionality of lift to the square of flow velocity.

The effects of flaps on the lift and drag coefficients are shown in Fig. 15–44 for an airfoil. Note that the maximum lift coefficient increases from about 1.5 for the airfoil with no flaps to 3.5 for the double-slotted flap case. But also
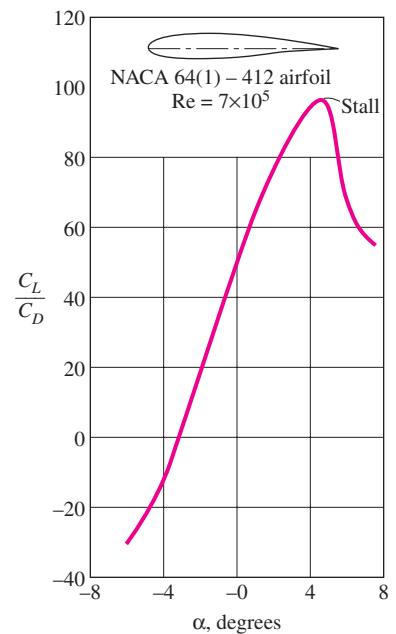
FIGURE 15–42
The variation of the lift-to-drag ratio with angle of attack for a two-dimensional airfoil (from Abbott, von Doenhoff, and Stivers).

(*a*) Flaps extended (takeoff)   (*b*) Flaps retracted (cruising)

FIGURE 15–43
The lift and drag characteristics of an airfoil during takeoff and landing can be changed by changing the shape of the airfoil by the use of movable flaps.
(© Yunus Çengel)

FIGURE 15–44
Effect of flaps on the lift and drag coefficients of an airfoil (from Abbott and von Doenhoff, Ref. 2, for NACA 23012).

Wing

Slot

Flap

FIGURE 15–45
A flapped airfoil with a slot
to increase the lift coefficient.

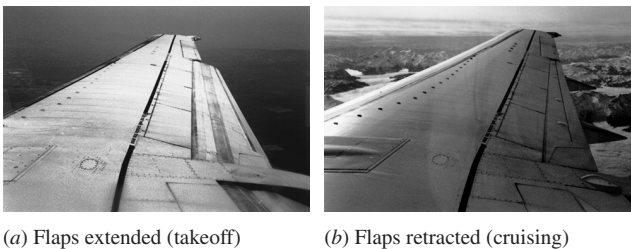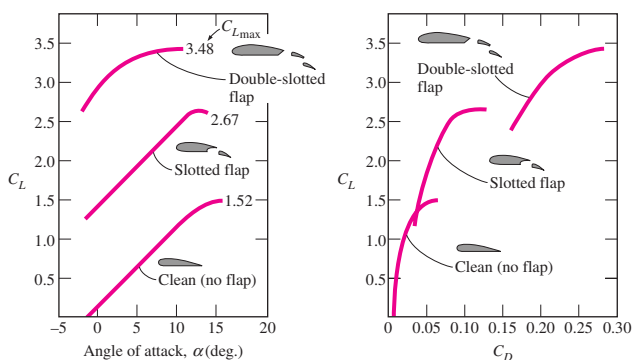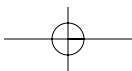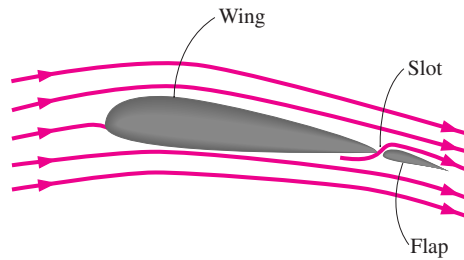note that the maximum drag coefficient increases from about 0.06 for the air-foil with no flaps to about 0.3 for the double-slotted flap case. This is a five-fold increase in the drag coefficient, and the engines must work much harder to provide the necessary thrust to overcome this drag. The angle of attack of the flaps can be increased to maximize the lift coefficient. Also, the leading and trailing edges extend the chord length, and thus enlarge the wing area A. The Boeing 727 uses a triple-slotted flap at the trailing edge and a slot at the leading edge.

The minimum flight velocity can be determined from the requirement that the total weight W of the aircraft be equal to lift and $C_L = C_{L,\,max}$. That is,

$$W = F_L = \tfrac{1}{2} C_{L,\,max} \, \rho \mathcal{V}^2_{min} \, A \qquad \rightarrow \qquad \mathcal{V}_{min} = \sqrt{\frac{2W}{\rho C_{L,\,max} A}} \qquad \text{(15–24)}$$

For a given weight, the landing or takeoff speed can be minimized by maximizing the product of the lift coefficient and the wing area, $C_{L,\,max} A$. One way of doing that is to use flaps, as already discussed. Another way is to control the boundary layer, which can be accomplished simply by leaving flow sections (slots) between the flaps, as shown in Fig. 15–45. Slots are used to prevent the separation of the boundary layer from the upper surface of the wings and the flaps. This is done by allowing air to move from the high-pressure region under the wing into the low-pressure region at the top surface. Note that the lift coefficient reaches its maximum value $C_L = C_{L,\,max}$, and thus the flight velocity reaches its minimum, at stall conditions, which is a region of unstable operation and must be avoided. The Federal Aviation Administration (FAA) does not allow operation below 1.2 times the stall speed for safety.

Another thing we notice from this equation is that the minimum velocity for takeoff or landing is inversely proportional to the square root of density. Noting that air density decreases with altitude (by about 15 percent at 1500 m), longer runways are required at airports at higher altitudes such as Denver to accommodate higher minimum takeoff and landing velocities. The situation becomes even more critical on hot summer days since the density of air is inversely proportional to temperature.

End Effects of Wing Tips

For airplane wings and other airfoils of finite size, the end effects at the tips become important because of the fluid leakage between the lower and upper surfaces. The pressure difference between the lower surface (high-pressure region) and the upper surface (low-pressure region) drives the fluid at the tips upwards while the fluid is swept toward the back because of the relative motion between the fluid and the wing. This results in a swirling motion that

spirals along the flow, called the **tip vortex,** at the tips of both wings. Vortices are also formed along the airfoil between the tips of the wings. These distributed vortices collect toward the edges after being shed from the trailing edges of the wings and combine with the tip vortices to form two streaks of powerful **trailing vortices** along the tips of the wings (Figs. 15–46 and 15–47). Trailing vortices generated by large aircraft continue to exist for a long time for long distances (over 10 km) before they gradually disappear due to viscous dissipation. Such vortices and the accompanying downdraft are strong enough to cause a small aircraft to lose control and flip over. Therefore, following a large aircraft closely (within 10 km) poses a real danger for smaller aircraft. In nature, this effect is used to advantage by birds that migrate in V-formation by utilizing the updraft generated by the bird in front. It has been determined that the birds in a typical flock can fly to their destination in V-formation with one-third less energy. Military jets also occasionally fly in V-formation for the same reason.

Tip vortices that interact with the free stream impose forces on the wing tips in all directions, including the flow direction. The component of the force in the flow direction adds to drag and is called **induced drag.** The total drag of a wing is then the sum of the induced drag (3-D effects) and the drag of the airfoil section.

The ratio of the square of the average span of an airfoil to the planform area is call the **aspect ratio.** For an airfoil with a rectangular planform of chord c and span $b,$ it is expressed as

$$AR = \frac{b^2}{A} = \frac{b^2}{bc} = \frac{b}{c}$$ (15–25)

Therefore, the aspect ratio is a measure of how narrow an airfoil is in the flow direction. The lift coefficient of wings, in general, increases while the drag coefficient decreases with increasing aspect ratio. This is because a long narrow wing (large aspect ratio) has a shorter tip length and thus smaller tip losses and smaller induced drag than a short and wide wing of the same planform area. Therefore, bodies with large aspect ratios fly more efficiently, but they are less maneuverable because of their larger moment of inertia (owing to the greater distance from the center). Bodies with smaller aspect ratios maneuver better since the wings are closer to the central part. So it is no surprise that *fighter*
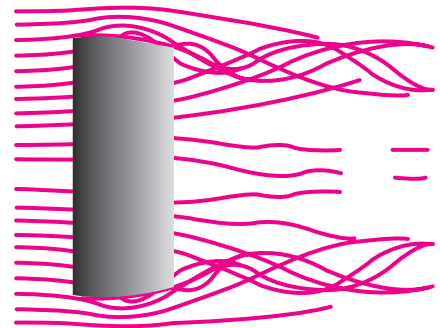

FIGURE 15–46
Trailing vortices from a rectangular wing with vortex cores leaving the trailing edge at the tips.

FIGURE 15–47
A crop duster flies through smoky air to illustrate the tip vortices produced at the tips of the wing. (NASA Langley Research Center)

(*a*) A bird with its wing tip feathers fanned out

FIGURE 15–48
Induced drag is reduced by
(*a*) wing tip feathers on bird wings
and (*b*) endplates or other disruptions
on airplane wings.

(*b*) Winglets are used on this sailplane to reduce induced drag. (Courtesy Schempp-Hirth)

planes (and fighter birds like falcons) have short and wide wings while *large commercial planes* (and soaring birds like albatrosses) have long and narrow wings.

The end effects can be minimized by attaching **endplates** at the tips of the wings perpendicular to the top surface. The endplates function by blocking some of the leakage around the wing tips, which results in considerable reduction in the strength of the tip vortices and the induced drag. Wing tip feathers on birds fan out for the same purpose (Fig. 15–48).

The development of efficient (low-drag) airfoils was the subject of intense experimental investigations in the 1930s. These airfoils were standardized by the National Advisory Committee for Aeronautics (NACA, which is now NASA), and extensive lists of data on lift coefficients were reported. The variation of the lift coefficient C_L with the angle of attack for two airfoils (NACA 0012 and NACA 2412) is given in Fig. 15–49. We make the following observations from this figure:

• The lift coefficient increases almost linearly with the angle of attack α, reaches a maximum at about $\alpha = 16°$, and then starts to decrease sharply. This decrease of lift with further increase in the angle of attack is called *stall,* and it is caused by flow separation and the formation of a wide wake region over the top surface of the airfoil. Stall is highly undesirable since it also increases drag.
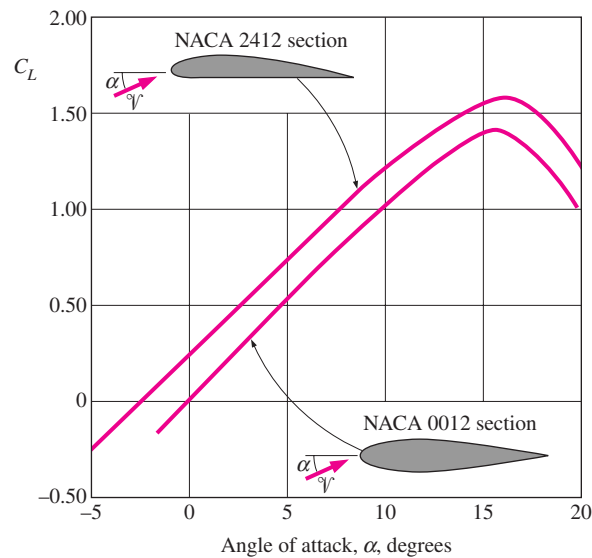
FIGURE 15–49
The variation of the lift coefficient with the angle of attack for a symmetrical and a nonsymmetrical airfoil (from Abbott).
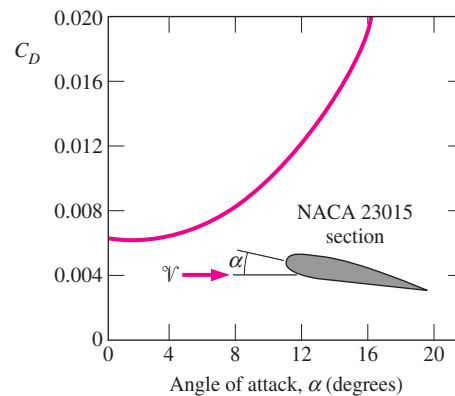
FIGURE 15–50
The variation of the drag coefficient of an airfoil with the angle of attack (from Abbott and von Doenhoff).

- At zero angle of attack ($\alpha = 0°$), the lift coefficient is zero for symmetrical airfoils but nonzero for nonsymmetrical ones with greater curvature at the top surface. Therefore, planes with symmetrical wing sections must fly with their wings at higher angles of attack in order to produce the same lift.
- The lift coefficient can be increased by severalfold by adjusting the angle of attack (from 0.25 at $\alpha = 0°$ for the nonsymmetrical airfoil to 1.25 at $\alpha = 10°$).
- The drag coefficient also increases with the angle of attack, often exponentially (Fig. 15–50). Therefore, large angles of attack should be used sparingly for short periods of time for fuel efficiency.

Lift Generated by Spinning

You have probably experienced giving a spin to a tennis ball or making a drop shot on a tennis or ping-pong ball by giving a fore spin in order to alter the lift characteristics and cause the ball to produce a more desirable trajectory and bounce of the shot. Golf, soccer, and baseball players also utilize spin in their
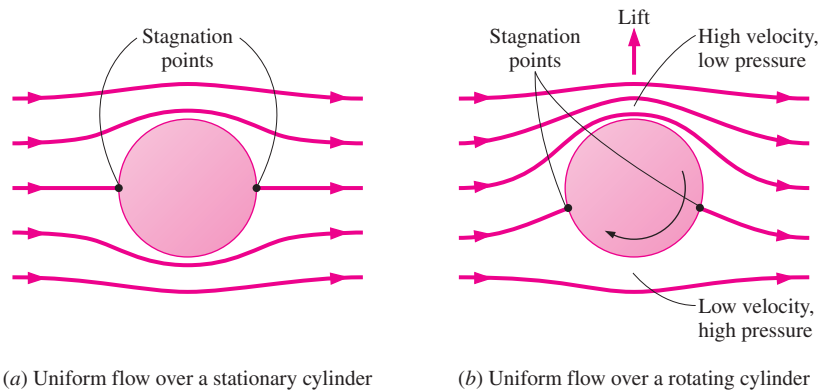
FIGURE 15–51
Generation of lift in uniform flow through rotation during "idealized" potential flow (the actual flow involves flow separation in the waste region).

(*a*) Uniform flow over a stationary cylinder   (*b*) Uniform flow over a rotating cylinder
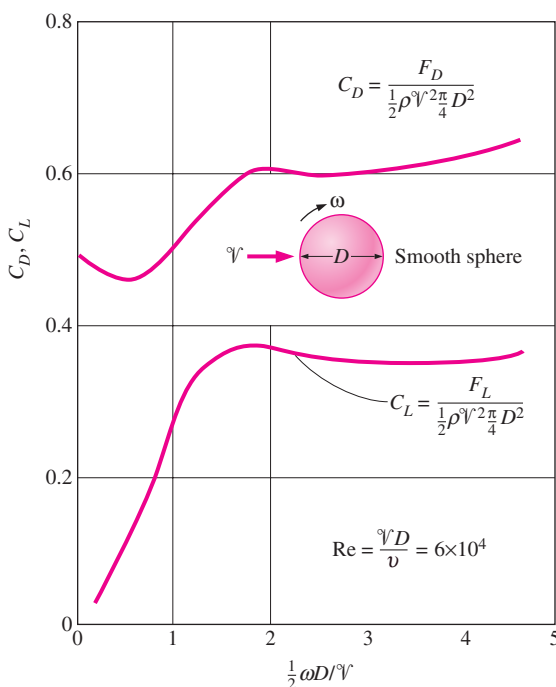
FIGURE 15–52
The variation of lift and drag coefficients of a smooth sphere with the rate of rotation for $Re = \mathcal{V}D/\nu = 6 \times 10^4$ (from Goldstein).

$$C_D = \frac{F_D}{\frac{1}{2}\rho \mathcal{V}^2 \frac{\pi}{4} D^2}$$

$$C_L = \frac{F_L}{\frac{1}{2}\rho \mathcal{V}^2 \frac{\pi}{4} D^2}$$

$$Re = \frac{\mathcal{V}D}{\upsilon} = 6 \times 10^4$$

games. The phenomenon of producing lift by the rotation of a solid body is called the **Magnus effect** after the German scientist Heinrich Magnus (1802–1870), who was the first to study the lift of rotating bodies, which is illustrated in Fig. 15–51. When the ball is not spinning, the lift is zero because of top-bottom symmetry. But when the cylinder is rotated about its axis, the cylinder drags some fluid around because of the no-slip condition and the flow field reflects the superposition of the spinning and nonspinning flows. The stagnation points shift down, and the flow is no longer symmetric about the horizontal plane that passes through the center of the cylinder. The average pressure on the upper half is less than the average pressure at the lower half because of the Bernoulli effect, and thus there is a *net upward force* (lift) acting on the cylinder. A similar argument can be given for the lift generated on a spinning ball.

The effect of the rate of rotation on the lift and drag coefficients of a smooth sphere is shown in Fig. 15–52. Note that the lift coefficient strongly depends

on the rate of rotation, especially at low angular velocities. The effect of the rate of rotation on the drag coefficient is small. Roughness also affects the drag and lift coefficients. In a certain range of the Reynolds number, roughness produces the desirable effect of increasing the lift coefficient while decreasing the drag coefficient. Therefore, golf balls with the right amount of roughness travel higher and farther than smooth balls for the same hit.

70,000 kg

150 m², double-flapped

558 km/h   12,000 m

FIGURE 15–53
Schematic for Example 15–5.

EXAMPLE 15–5   Lift and Drag of a Commercial Airplane

A commercial airplane has a total mass of 70,000 kg and a wing planform area of 150 m² (Fig. 15–53). The plane has a cruising speed of 558 km/h and a cruising altitude of 12,000 m, where the air density is 0.312 kg/m³. The plane has double-slotted flaps for use during takeoff and landing, but it cruises with all flaps retracted. Assuming the lift and the drag characteristics of the wings can be approximated by NACA 23012 (Fig. 15–44), determine (*a*) the minimum safe speed for takeoff and landing with and without extending the flaps, (*b*) the angle of attack to cruise steadily at the cruising altitude, and (*c*) the power that needs to be supplied to provide enough thrust to overcome wing drag.

SOLUTION   The cruising conditions of a passenger plane and its wing characteristics are given. The minimum safe landing and takeoff speeds, the angle of attack during cruising, and the power required are to be determined.
Assumptions   **1** The drag and lift produced by parts of the plane other than the wings, such as the fuselage drag, are not considered. **2** The wings are assumed to be two-dimensional airfoil sections, and the tip effects of the wings are not considered. **3** The lift and the drag characteristics of the wings can be approximated by NACA 23012 so that Fig. 15–44 is applicable. **4** The average density of air on the ground is 1.20 kg/m³.
Properties   The densities of air are 1.20 kg/m³ on the ground and 0.312 kg/m³ at cruising altitude. The maximum lift coefficients $C_{L, max}$ of the wings are 3.48 and 1.52 with and without flaps, respectively (Fig. 15–44).
Analysis   (*a*) The weight and cruising speed of the airplane are

$$W = mg = (70{,}000 \text{ kg})(9.81 \text{ m/s}^2)\left(\frac{1 \text{ N}}{1 \text{ kg} \cdot \text{m/s}^2}\right) = 686{,}700 \text{ N}$$

$$\mathcal{V} = (558 \text{ km/h})\left(\frac{1 \text{ m/s}}{3.6 \text{ km/h}}\right) = 155 \text{ m/s}$$

The minimum velocity corresponding to the stall conditions without and with flaps are

$$\mathcal{V}_{min \, 1} = \sqrt{\frac{2W}{\rho C_{L, max \, 1}A}} = \sqrt{\frac{2(686{,}700 \text{ N})}{(1.2 \text{ kg/m}^3)(1.52)(150 \text{ m}^3)}\left(\frac{1 \text{ kg} \cdot \text{m/s}^2}{1 \text{ N}}\right)} = 70.9 \text{ m/s}$$

$$\mathcal{V}_{min \, 2} = \sqrt{\frac{2W}{\rho C_{L, max \, 2}A}} = \sqrt{\frac{2(686{,}700 \text{ N})}{(1.2 \text{ kg/m}^3)(3.48)(150 \text{ m}^2)}\left(\frac{1 \text{ kg} \cdot \text{m/s}^2}{1 \text{ N}}\right)} = 46.8 \text{ m/s}$$

Then the "safe" minimum velocities to avoid the stall region are obtained by multiplying the values above by 1.2:

Without flaps: $\mathcal{V}_{min \, 1, safe} = 1.2\mathcal{V}_{min \, 1} = 1.2 \times (70.9 \text{ m/s}) = 85.1 \text{ m/s} = $ **306 km/h**
With flaps: $\mathcal{V}_{min \, 2, safe} = 1.2\mathcal{V}_{min \, 2} = 1.2 \times (46.8 \text{ m/s}) = 56.2 \text{ m/s} = $ **202 km/h**
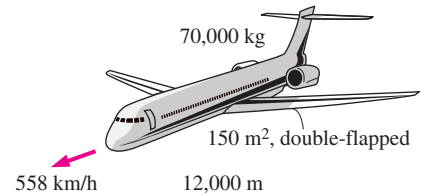
since 1 m/s = 3.6 km/h. Note that the use of flaps allows the plane to take off and land at considerably lower velocities, and thus on a shorter runway.

(*b*) When an aircraft is cruising steadily at a constant altitude, the lift must be equal to the weight of the aircraft, $F_L = W$. Then the lift coefficient is determined to be

$$C_L = \frac{F_L}{\frac{1}{2}\rho V^2 A} = \frac{686{,}700 \text{ N}}{\frac{1}{2}(0.312 \text{ kg/m}^3)(155 \text{ m/s})^2(150 \text{ m}^2)}\left(\frac{1 \text{ kg} \cdot \text{m/s}^2}{1 \text{ N}}\right) = 1.22$$

For the case of no flaps, the angle of attack corresponding to this value of C_L is determined from Fig. 15–44 to be $\alpha \approx \mathbf{10°.}$

(*c*) When the aircraft is cruising steadily at a constant altitude, the net force acting on the aircraft is zero, and thus thrust provided by the engines must be equal to the drag force. The drag coefficient corresponding to the cruising lift coefficient of 1.22 is determined from Fig. 15–44 to be $C_D \approx 0.03$. Then the drag force acting on the wings becomes

$$F_D = C_D A \frac{\rho V^2}{2} = (0.03)(150 \text{ m}^2)\frac{(0.312 \text{ kg/m}^3)(155 \text{ m/s})^2}{2}\left(\frac{1 \text{ kN}}{1000 \text{ kg} \cdot \text{m/s}^2}\right) = 16.9 \text{ kN}$$

Noting that power is force times velocity (distance per unit time), the power required to overcome this drag is equal to the thrust times the cruising velocity:

$$\text{Power} = \text{Thrust} \times \text{Velocity} = F_D V = (16.9 \text{ kN})(155 \text{ m/s})\left(\frac{1 \text{ kW}}{1 \text{ kN} \cdot \text{m/s}}\right) = \mathbf{2620 \text{ kW}}$$

Therefore, the engines must supply 2620 kW of power to overcome the drag during cruising. For a propulsion efficiency of 30 percent (i.e., 30 percent of the energy of the fuel is utilized to propel the aircraft), the plane requires energy input at a rate of 8733 kJ/s.

Discussion The power determined above is the power to overcome the drag that acts on the wings only and does not include the drag that acts on the remaining parts of the aircraft (the fuselage, the tail, etc.). Therefore, the total power required during cruising will be much greater. Also, it does not consider induced drag which can be dominant during takeoff when the angle of attack is high (Fig. 15–44 is for a 2-D airfoil, and does not include 3-D effects).
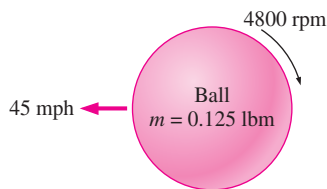

EXAMPLE 15–6   Effect of Spin on a Tennis Ball

A tennis ball with a mass of 0.125 lbm and a diameter of 2.52 in is hit at 45 mph with a backspin of 4800 rpm (Fig. 15–54). Determine if the ball will fall or rise under the combined effect of gravity and lift due to spinning shortly after being hit in air at 1 atm and 80°F.

SOLUTION   A tennis ball is hit with a backspin. It is to be determined whether the ball will fall or rise after being hit.

Assumptions   **1** The surfaces of the ball are smooth enough for Fig. 15–52 to be applicable. **2** The ball is hit horizontally so that it starts its motion horizontally.

Properties   The density and kinematic viscosity of air at 1 atm and 80°F are $\rho = 0.07350$ lbm/ft³ and $v = 0.6110$ ft²/h = (Table A–22E).

4800 rpm

45 mph ← Ball
$m = 0.125$ lbm

FIGURE 15–54
Schematic for Example 15–6.

Analysis   The ball is hit horizontally, and thus it would normally fall under the effect of gravity without the spin. The backspin generates a lift, and the ball will rise if the lift is greater than the weight of the ball. The lift can be determined from

$$F_L = C_L A \frac{\rho \mathcal{V}^2}{2}$$

where A is the frontal area of the ball, which is $A = \pi D^2/4$. The translational and angular velocities of the ball are

$$\mathcal{V} = (45 \text{ mi/h})\left(\frac{5280 \text{ ft}}{1 \text{ mi}}\right)\left(\frac{1 \text{ h}}{3600 \text{ s}}\right) = 66 \text{ ft/s}$$

$$\omega = (4800 \text{ rev/min})\left(\frac{2\pi \text{ rad}}{1 \text{ rev}}\right)\left(\frac{1 \text{ min}}{60 \text{ s}}\right) = 502 \text{ rad/s}$$

Then,

$$\frac{\omega D}{2\mathcal{V}} = \frac{(502 \text{ rad/s})(2.52/12 \text{ ft})}{2(66 \text{ ft/s})} = 0.80 \text{ rad}$$

From Fig. 15–52, the lift coefficient corresponding to this value is $C_L = 0.21$. Then the lift acting on the ball is

$$F_L = (0.21) \frac{\pi(2.52/12 \text{ ft})^2}{4} \frac{(0.0735 \text{ lbm/ft}^3)(66 \text{ ft/s})^2}{2}\left(\frac{1 \text{ lbf}}{32.2 \text{ lbm} \cdot \text{ft/s}^2}\right) = 0.036 \text{ lbf}$$

The weight of the ball is

$$W = mg = (0.125 \text{ lbm})(32.2 \text{ ft/s}^2)\left(\frac{1 \text{ lbf}}{32.2 \text{ lbm} \cdot \text{ft/s}^2}\right) = 0.125 \text{ lbf}$$

which is more than the lift. Therefore, the ball will **drop** under the combined effect of gravity and lift due to spinning after hitting with a net force of $0.125 - 0.036 = 0.089$ lbf.

Discussion   This example shows that the ball can be hit much farther by giving it a backspin. Note that a topspin has the opposite effect (negative lift) and speeds up the drop of the ball to the ground. Also, the Reynolds number for this problem is 8×10^4, which is sufficiently close to the 6×10^4 for which Fig. 15–52 is prepared.

SUMMARY

In this chapter, we studied flow of fluids over immersed bodies with emphasis on the resulting lift and drag forces. A fluid may exert forces and moments on a body in and about various directions. The force a flowing fluid exerts on a body in the flow direction is called *drag*. The components of the pressure and wall shear forces in the normal direction to flow tend to move the body in that direction and are called *lift*. The part of drag that is due directly to wall shear stress τ_w is called the *skin friction drag* since it is caused by frictional effects, and the part that is due directly to pressure P is called the *pressure drag* or *form drag* because of its strong dependence on the form or shape of the body.

The *drag coefficient* C_D and the *lift coefficient* C_L are dimensionless numbers that represent the drag and the lift characteristics of a body and are defined as

$$C_D = \frac{F_D}{\frac{1}{2}\rho \mathcal{V}^2 A} \qquad \text{and} \qquad C_L = \frac{F_L}{\frac{1}{2}\rho \mathcal{V}^2 A}$$

where A is usually the *frontal area* (the area projected on a plane normal to the direction of flow) of the body. For plates and airfoils, A is taken to be the *planform area*, which is the area that would be seen by a person looking at the body from above in a direction normal to the body. The drag coefficient, in general, depends on the *Reynolds number*, especially for Reynolds numbers below 10^4. At higher Reynolds numbers, the drag coefficients for most geometries remain essentially constant.

A body is said to be *streamlined* if a conscious effort is made to align its shape with the anticipated streamlines in the flow in order to reduce drag. Otherwise, a body (such as a building) tends to block the flow and is said to be *blunt* or *bluff*. At sufficiently high velocities, the fluid stream detaches itself from the surface of the body. This is called *flow separation*. When a fluid stream separates from the body, it forms a *separated region* between the body and the fluid stream. Separation also may occur on a streamlined body such as an airplane wing at a sufficiently large *angle of attack*, which is the angle the incoming fluid stream makes with the *chord* (the line that connects the nose and the end) of the body. Flow separation on the top surface of a wing reduces lift drastically and may cause the airplane to *stall*.

The region of flow above a surface bounded by δ_v in which the effects of the viscous shearing forces caused by fluid viscosity are felt is called the *velocity boundary layer* or just the *boundary layer*. The *thickness* of the boundary layer, δ, is defined as the distance from the surface at which the velocity is $0.99\mathcal{V}$. The hypothetical line of velocity $0.99\mathcal{V}$ divides the flow over a plate into two regions: the *boundary layer region*, in which the viscous effects and the velocity changes are significant, and the *irrotational outer flow region*, in which the frictional effects are negligible and the velocity remains essentially constant.

For external flow, the Reynolds number is expressed as

$$\text{Re}_L = \frac{\rho \mathcal{V} L}{\mu} = \frac{\mathcal{V} L}{\upsilon}$$

where $\mathcal{V}$ is the upstream velocity and L is the characteristic length of the geometry, which is the length of the plate in the flow direction for a flat plate and the diameter D for a cylinder or sphere. The *average* friction coefficients over an entire flat plate are

Laminar flow: $\qquad C_f = \dfrac{1.328}{\text{Re}_L^{1/2}} \qquad \text{Re}_L < 5 \times 10^5$

Turbulent flow: $\qquad C_f = \dfrac{0.074}{\text{Re}_L^{1/5}} \qquad 5 \times 10^5 \leq \text{Re}_L \leq 10^7$

The first relation gives the average friction coefficient for the entire plate when the flow is laminar over the entire plate. For a critical Reynolds number of $\text{Re}_{cr} = 5 \times 10^5$, the average friction coefficient over an *entire* flat plate is

$$C_f = \frac{0.074}{\text{Re}_L^{1/5}} - \frac{1742}{\text{Re}_L} \qquad 5 \times 10^5 \leq \text{Re}_L \leq 10^7$$

A curve fit of experimental data for the average friction coefficient in this regime is

Rough surface: $\qquad C_f = \left(1.89 - 1.62 \log \dfrac{\varepsilon}{L} \right)^{-2.5}$

where ε is the surface roughness and L is the length of the plate in the flow direction. In the absence of a better relation, the relation above can be used for turbulent flow on rough surfaces for $\text{Re} > 10^6$, especially when $\varepsilon/L > 10^{-4}$.

Surface roughness, in general, increases the drag coefficient in turbulent flow. For blunt bodies such as a circular cylinder or sphere, however, an increase in the surface roughness may *decrease* the drag coefficient. This is done by tripping the flow into turbulence at a lower Reynolds number, and thus causing the fluid to close in behind the body, narrowing the wake and reducing pressure drag considerably. It is desirable for airfoils to generate the most lift while producing the least drag. Therefore, a measure of performance for airfoils is the *lift-to-drag ratio*, C_L/C_D.

The minimum flight velocity of an aircraft can be determined from

$$\mathcal{V}_{\min} = \sqrt{\frac{2W}{\rho C_{L,\max} A^*}}$$

For a given weight, the landing or takeoff speed can be minimized by maximizing the product of the lift coefficient and the wing area, $C_{L,\max} A$. For airplane wings and other airfoils of finite size, the pressure difference between the lower and the upper surfaces drives the fluid at the tips upward. This results in a swirling motion that spirals along the flow, called the *tip vortex*. Tip vortices that interact with the free stream impose forces on the wing tips in all directions, including the flow direction. The component of the force in the flow direction adds to drag and is called *induced drag*. The total drag of a wing is then the sum of the induced drag (3-D effects) and the drag of the airfoil section. It is observed that lift develops when a cylinder or sphere in flow is rotated at a sufficiently high rate. The phenomenon of producing lift by the rotation of a solid body is called the *Magnus effect*.

REFERENCES AND SUGGESTED READING

1. I. H. Abbott. "The Drag of Two Streamline Bodies as Affected by Protuberances and Appendages." *NACA Report* 451, 1932.

2. I. H. Abbott and A. E. von Doenhoff. *Theory of Wing Sections, Including a Summary of Airfoil Data*. New York: Dover, 1959.

3. I. H. Abbott, A. E. von Doenhoff, and L. S. Stivers. "Summary of Airfoil Data." *NACA Report* 824, Langley Field, VA, 1945.

4. J. D. Anderson. *Fundamentals of Aerodynamics*. 2nd ed. New York: McGraw-Hill, 1991.

5. R. D. Blevins. *Applied Fluid Dynamics Handbook*. New York: Van Nostrand Reinhold, 1984.

6. S. W. Churchill and M. Bernstein. "A Correlating Equation for Forced Convection from Gases and Liquids to a Circular Cylinder in Cross Flow." *Journal of Heat Transfer* 99 (1977), pp. 300–6.

7. C. T. Crowe, J. A. Roberson, and D. F. Elger. *Engineering Fluid Mechanics.* 7th ed. New York: Wiley, 2001.

8. S. Goldstein. *Modern Developments in Fluid Dynamics*. London: Oxford Press, 1938.

9. J. Happel. *Low Reynolds Number Hydrocarbons*. Englewood Cliffs, NJ: Prentice Hall, 1965.

10. S. F. Hoerner. *Fluid-Dynamic Drag.* [Published by the author.] Library of Congress No. 64, 1966.

11. G. M. Homsy, H. Aref, K. S. Breuer, S. Hochgreb, J. R. Koseff, B. R. Munson, K. G. Powell, C. R. Robertson, S. T. Thoroddsen. *Multi-Media Fluid Mechanics* (CD). Cambridge University Press.

12. W. H. Hucho. *Aerodynamics of Road Vehicles*. London: Butterworth-Heinemann, 1987.

13. B. R. Munson, D. F. Young, and T. Okiishi. *Fundamentals of Fluid Mechanics.* 4th ed. New York: Wiley, 2002.

14. M. C. Potter and D. C. Wiggert. *Mechanics of Fluids*. 2nd ed. Upper Saddle River, NJ: Prentice Hall, 1997.

15. C. T. Crowe, J. A. Roberson, and D. F. Elger. *Engineering Fluid Mechanics.* 7th ed. New York: Wiley, 2001.

16. H. Schlichting. *Boundary Layer Theory.* 7th ed. New York: McGraw-Hill, 1979.

17. M. Van Dyke. *An Album of Fluid Motion.* Stanford, CA: The Parabolic Press, 1982.

18. J. Vogel. *Life in Moving Fluids.* 2nd ed. Boston: Willard Grand Press, 1994.

19. F. M. White. *Fluid Mechanics.* 5th ed. New York: McGraw-Hill, 2003.

PROBLEMS*

Drag, Lift, and Drag Coefficients of Common Geometries

15–1C Explain when an external flow is two-dimensional, three-dimensional, and axisymmetric. What type of flow is the flow of air over a car?

15–2C What is the difference between the upstream velocity and the free-stream velocity? For what types of flow are these two velocities equal to each other?

15–3C What is the difference between streamlined and blunt bodies? Is a tennis ball a streamlined or blunt body?

15–4C What is cavitation? Under what conditions does it occur? Why do we try to avoid cavitation?

*Problems designated by a "C" are concept questions, and students are encouraged to answer them all. Problems designated by an "E" are in English units, and the SI users can ignore them. Problems with a CD-EES icon ⊛ are solved using EES, and complete solutions together with parametric studies are included on the enclosed CD. Problems with a computer-EES icon ▣ are comprehensive in nature, and are intended to be solved with a computer, preferably using the EES software that accompanies this text.

15–5C What is drag? What causes it? Why do we usually try to minimize it?

15–6C What is lift? What causes it? Does wall shear contribute to the lift?

15–7C During flow over a given body, the drag force, the upstream velocity, and the fluid density are measured. Explain how you would determine the drag coefficient. What area would you use in calculations?

15–8C During flow over a given slender body such as a wing, the lift force, the upstream velocity, and the fluid density are measured. Explain how you would determine the lift coefficient. What area would you use in calculations?

15–9C Define frontal area of a body subjected to external flow. When is it appropriate to use the frontal area in drag and lift calculations?

15–10C Define planform area of a body subjected to external flow. When is it appropriate to use the planform area in drag and lift calculations?

15–11C What is terminal velocity? How is it determined?

15–12C What is the difference between skin friction drag and pressure drag? Which is usually more significant for slender bodies such as airfoils?

15–13C What is the effect of surface roughness on the friction drag coefficient in laminar and turbulent flows?

15–14C In general, how does the drag coefficient vary with the Reynolds number at (a) low and moderate Reynolds numbers and (b) at high Reynolds numbers (Re $>$ 10⁴)?

15–15C Fairings are attached to the front and back of a cylindrical body to make it look like an airfoil. What is the effect of this modification on the (a) friction drag, (b) pressure drag, and (c) total drag? Assume the Reynolds number is high enough so that the flow is turbulent for both cases.
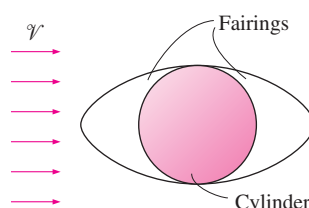
FIGURE P15–15C

15–16C What is the effect of streamlining on (a) friction drag and (b) pressure drag? Does the total drag acting on a body necessarily decrease as a result of streamlining? Explain.

15–17C What is flow separation? What causes it? What is the effect of flow separation on the drag coefficient?

15–18C What is drafting? How does it affect the drag coefficient of the drafted body?

15–19C Which car is more likely to be more fuel-efficient: the one with sharp corners or the one that is contoured to resemble an ellipse? Why?

15–20C Which bicyclist is more likely to go faster: the one who keeps his head and his body in the most upright position or the one who leans down and brings his body closer to his knees? Why?

15–21 The drag coefficient of a car at the design conditions of 1 atm, 25°C, and 90 km/h is to be determined experimentally in a large wind tunnel in a full-scale testing. The height and width of the car are 1.40 m and 1.65 m, respectively. If the horizontal force acting on the car is measured to be 300 N, determine the total drag coefficient of this car. *Answer:* 0.35

15–22 A car is moving at a constant velocity of 80 km/h. Determine the upstream velocity to be used in fluid flow analysis if (a) the air is calm, (b) wind is blowing against the direction of motion of the car at 30 km/h, and (c) wind is blowing in the same direction of motion of the car at 50 km/h.

15–23 The resultant of the pressure and wall shear forces acting on a body is measured to be 700 N, making 35° with the direction of flow. Determine the drag and the lift forces acting on the body.
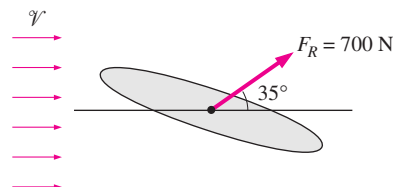

FIGURE P15–23

15–24 During a high Reynolds number experiment, the total drag force acting on a spherical body of diameter $D = 12$ cm subjected to air flow at 1 atm and 5°C is measured to be 5.2 N. The pressure drag acting on the body is calculated by integrating the pressure distribution (measured by the use of pressure sensors throughout the surface) to be 4.9 N. Determine the friction drag coefficient of the sphere.
Answer: 0.0115

15–25E To reduce the drag coefficient and thus to improve the fuel efficiency, the frontal area of a car is to be reduced. Determine the amount of fuel and money saved per year as a result of reducing the frontal area from 18 ft² to 15 ft². Assume the car is driven 12,000 miles a year at an average speed of 55 mph. Take the density and price of gasoline to be 50 lbm/ft³ and \$2.20/gal, respectively; the density of air to be 0.075 lbm/ft³, the heating value of gasoline to be 20,000 Btu/lbm; and the overall efficiency of the engine to be 32 percent.

15–26E Reconsider Prob. 15–25E. Using EES (or other) software, investigate the effect of frontal area on the annual fuel consumption of the car. Let the frontal area vary from 10 to 30 ft² in increments of 2 ft². Tabulate and plot the results.

15–27 A circular stop sign has a diameter of 50 cm and is subjected to winds up to 150 km/h at 10°C and 100 kPa. Determine the drag force acting on the sign. Also determine the bending moment at the bottom of its pole whose height from the ground to the bottom of the sign is 1.5 m. Disregard the drag on the pole.
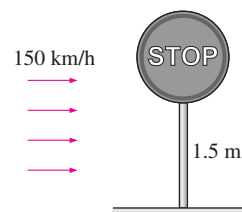

FIGURE P15–27

15–28E Wind loading is a primary consideration in the design of the supporting mechanisms of billboards, as evidenced by many billboards being knocked down during high winds. Determine the wind force acting on an 8-ft-high 20-ft-wide

billboard due to 90-mph winds in the normal direction when the atmospheric conditions are 14.3 psia and 40°F.
Answer: 6684 lbf

15–29 Advertisement signs are commonly carried by taxicabs for additional income, but they also increase the fuel cost. Consider a sign that consists of a 0.30-m-high, 0.9-m-wide, and 0.9-m-long rectangular block mounted on top of a taxicab such that the sign has a frontal area of 0.3 m by 0.9 m from all four sides. Determine the increase in the annual fuel cost of this taxicab due to this sign. Assume the taxicab is driven 60,000 km a year at an average speed of 50 km/h and the overall efficiency of the engine is 28 percent. Take the density, unit price, and heating value of gasoline to be 0.75 kg/L, $0.50/L, and 42,000 kJ/kg, respectively, and the density of air to be 1.25 kg/m^3.

FIGURE P15–29

15–30 It is proposed to meet the water needs of a recreational vehicle (RV) by installing a 2-m-long, 0.5-m-diameter cylindrical tank on top of the vehicle. Determine the additional power requirement of the RV at a speed of 95 km/h when the tank is installed such that its circular surfaces face (*a*) the front and back and (*b*) the sides of the RV. Assume atmospheric conditions are 87 kPa and 20°C.   *Answers:* (*a*) 1.67 kW, (*b*) 7.55 kW
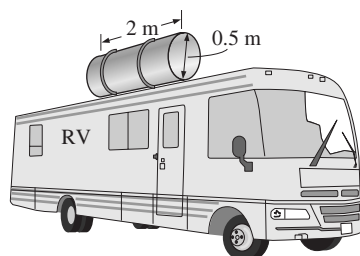

FIGURE P15–30

15–31E At highway speeds, the power generated by car engines is mostly used to overcome aerodynamic drag, and thus the fuel consumption is nearly proportional to the drag force on a level road. Determine the percentage increase in fuel consumption of a car per unit time when a person who normally drives at 55 mph now starts driving at 75 mph.

15–32 A 4-mm-diameter plastic sphere whose density is 1150 kg/m^3 is dropped into water at 20°C. Determine the terminal velocity of the sphere in water.

15–33 During major windstorms, high vehicles such as RVs and semitrucks may be thrown off the road and boxcars off their tracks, especially when they are empty and in open areas.

Consider a 5000-kg semitruck that is 8 m long, 2 m high, and 2 m wide. The distance between the bottom of the truck and the road is 0.75 m. Now the truck is exposed to winds from its side surface. Determine the wind velocity that will tip the truck over to its side. Take the air density to be 1.1 kg/m^3.
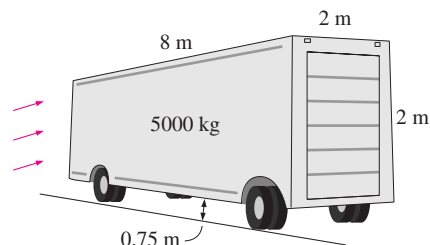

FIGURE P15–33

15–34 An 80-kg bicyclist is riding his 15-kg bicycle downhill on a road with a slope of 12° without pedaling or breaking. The bicyclist has a frontal area of 0.45 m^2 and a drag coefficient of 1.1 in the upright position, and a frontal area of 0.4 m^2 and a drag coefficient of 0.9 in the racing position. Disregarding the rolling resistance and friction at the bearings, determine the terminal velocity of the bicyclist for both positions. Take the air density to be 1.25 kg/m^3.   *Answers:* 90 km/h, 106 km/h

15–35 A wind turbine with two or four hollow hemispherical cups connected to a pivot is commonly used to measure wind speed. Consider a wind turbine with two 8-cm-diameter cups with a center-to-center distance of 25 cm, as shown in the figure. The pivot is stuck as a result of some malfunction, and the cups stopped rotating. For a wind speed of 15 m/s and air density of 1.25 kg/m^3, determine the maximum torque this turbine applies on the pivot.
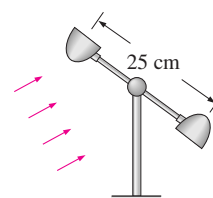

FIGURE P15–35

15–36 Reconsider Prob. 15–35. Using EES (or other) software, investigate the effect of wind speed on the torque applied on the pivot. Let the wind speed vary from 0 to 50 m/s in increments of 5 m/s. Tabulate and plot the results.

15–37E A 5-ft-diameter spherical tank completely submerged in fresh water is being towed by a ship at 12 ft/s. Assuming turbulent flow, determine the required towing power.

15–38 During steady motion of a vehicle on a level road, the power delivered to the wheels is used to overcome aerodynamic drag and rolling resistance (the product of the rolling resistance coefficient and the weight of the vehicle), assuming

the friction at the bearings of the wheels is negligible. Consider a car that has a total mass of 950 kg, a drag coefficient of 0.32, a frontal area of 1.8 m^2, and a rolling resistance coefficient of 0.04. The maximum power the engine can deliver to the wheels is 80 kW. Determine (*a*) the speed at which the rolling resistance is equal to the aerodynamic drag force and (*b*) the maximum speed of this car. Take the air density to be 1.20 kg/m^3.

15–39 Reconsider Prob. 15–38. Using EES (or other) software, investigate the effect of car speed on the required power to overcome (*a*) rolling resistance, (*b*) the aerodynamic drag, and (*c*) their combined effect. Let the car speed vary from 0 to 150 km/h in increments of 15 km/h. Tabulate and plot the results.

15–40 A submarine can be treated as an ellipsoid with a diameter of 5 m and a length of 25 m. Determine the power required for this submarine to cruise horizontally and steadily at 40 km/h in seawater whose density is 1025 kg/m^3. Also determine the power required to tow this submarine in air whose density is 1.30 kg/m^3. Assume the flow is turbulent in both cases.
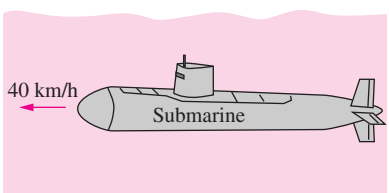

40 km/h

Submarine

FIGURE P15–40

15–41 An 0.80-m-diameter, 1.2-m-high garbage can is found in the morning tipped over due to high winds during the night. Assuming the average density of the garbage inside to be 150 kg/m^3 and and taking the air density to be 1.25 kg/m^3, estimate the wind velocity during the night when the can was tipped over. Take the drag coefficient of the can to be 0.7. *Answer: 186 km/h*

15–42E The drag coefficient of a vehicle increases when its windows are rolled down or its sunroof is opened. A sports car has a frontal area of 18 ft^2 and a drag coefficient of 0.32 when the windows and sunroof are closed. The drag coefficient in-
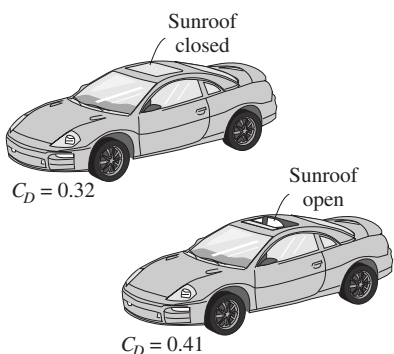

Sunroof closed

$C_D = 0.32$

Sunroof open

$C_D = 0.41$

FIGURE P15–42E

creases to 0.41 when the sunroof is open. Determine the additional power consumption of the car when the sunroof is opened at (*a*) 35 mph and (*b*) 70 mph. Take the density of air to be 0.075 lbm/ft^3.

Flow over Flat Plates

15–43C What fluid property is responsible for the development of the velocity boundary layer? For what kind of fluids will there be no velocity boundary layer on a flat plate?

15–44C What does the friction coefficient represent in flow over a flat plate? How is it related to the drag force acting on the plate?

15–45C Consider laminar flow over a flat plate. Will the friction coefficient change with position?

15–46C How is the average friction coefficient determined in flow over a flat plate?

15–47E Light oil at 75°F flows over a 15-ft-long flat plate with a free-stream velocity of 6 ft/s. Determine the total drag force per unit width of the plate.

15–48 The local atmospheric pressure in Denver, Colorado (elevation 1610 m), is 83.4 kPa. Air at this pressure and at 25°C flows with a velocity of 6 m/s over a 2.5-m × 8-m flat plate. Determine the drag force acting on the top surface of the plate if the air flows parallel to the (*a*) 8-m-long side and (*b*) the 2.5-m-long side.

15–49 During a winter day, wind at 55 km/h and 5°C is blowing parallel to a 4-m-high and 10-m-long wall of a house. Assuming the wall surfaces to be smooth, determine the drag force acting on the wall. What would your answer be if the wind velocity has doubled? *Answers: 16 N, 58 N*
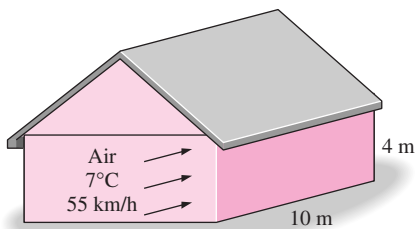

Air
7°C
55 km/h

4 m

10 m

FIGURE P15–49

15–50E Air at 70°F flows over a 10-ft-long flat plate at 25 ft/s. Determine the local friction coefficient at intervals of 1 ft and plot the results against the distance from the leading edge.

15–51 The forming section of a plastics plant puts out a continuous sheet of plastic that is 1.2 m wide and 2 mm thick at a rate of 15 m/min. The sheet is subjected to air flow at a velocity of 3 m/s on both sides along its surfaces normal to the direction of motion of the sheet. The width of the air cooling section is such that a fixed point on the plastic sheet passes through that section in 2 s. Using properties of air at 1 atm and 60°C, determine the drag force the air exerts on the plastic sheet in the direction of airflow.
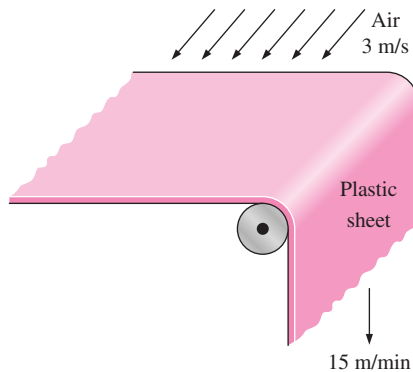
FIGURE P15–51

15–52 The top surface of the passenger car of a train moving at a velocity of 70 km/h is 3.2 m wide and 8 m long. If the outdoors air is at 1 atm and 25°C, determine the drag force acting on the top surface of the car.
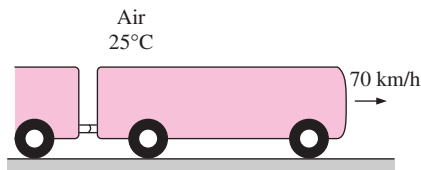

FIGURE P15–52

15–53 The weight of a thin flat plate 50 cm × 50 cm in size is balanced by a counterweight that has a mass of 2 kg, as shown in the figure. Now a fan is turned on, and air at 1 atm and 25°C flows downward over both surfaces of the plate with a free-stream velocity of 10 m/s. Determine the mass of the counterweight that needs to be added in order to balance the plate in this case.
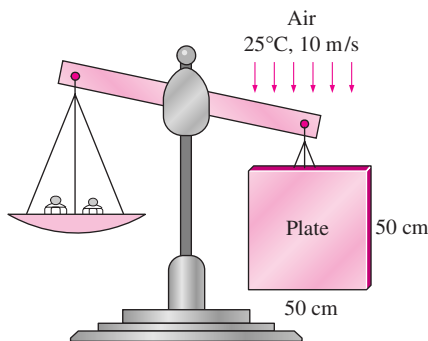
FIGURE P15–53

15–54 Consider laminar flow of a fluid over a flat plate. Now the free-stream velocity of the fluid is doubled. Determine the change in the drag force on the plate. Assume the flow to remain laminar. *Answer:* A 2.83-fold increase

15–55E Consider a refrigeration truck traveling at 65 mph at a location where the air temperature is at 1 atm and 80°F. The refrigerated compartment of the truck can be considered to be a 9-ft-wide, 8-ft-high, and 20-ft-long rectangular box. Assuming the airflow over the entire outer surface to be turbulent, determine the drag force acting on the top and side surfaces and the power required to overcome this drag.
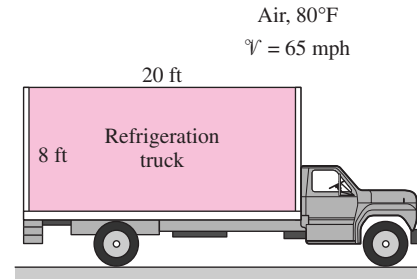

FIGURE P15–55E

15–56E Reconsider Prob. 15–55E. Using EES (or other) software, investigate the effect of truck speed on the total drag force acting on the top and side surfaces, and the power required to overcome it. Let the truck speed vary from 0 to 100 mph in increments of 10 mph. Tabulate and plot the results.

15–57 Air at 25°C and 1 atm is flowing over a long flat plate with a velocity of 8 m/s. Determine the distance from the leading edge of the plate where the flow becomes turbulent, and the thickness of the boundary layer at that location.

15–58 Repeat Prob. 15–57 for water.

Flow Across Cylinders and Spheres

15–59C In flow over cylinders, why does the drag coefficient suddenly drop when the flow becomes turbulent? Isn't turbulence supposed to increase the drag coefficient instead of decreasing it?

15–60C In flow over blunt bodies such as a cylinder, how does the pressure drag differ from the friction drag?

15–61C Why is flow separation in flow over cylinders delayed in turbulent flow?

15–62E A 1.2-in-outer-diameter pipe is to cross a river at a 105-ft-wide section while being completely immersed in water. The average flow velocity of water is 10 ft/s, and the water temperature is 70°F. Determine the drag force exerted on the pipe by the river. *Answer:* 1320 lbf

15–63 A long 8-cm-diameter steam pipe passes through some area open to the winds. Determine the drag force acting on the pipe per unit of its length when the air is at 1 atm and 5°C and the wind is blowing across the pipe at a velocity of 50 km/h.

15–64E A person extends his uncovered arms into the windy air outside at 1 atm and 60°F and 20 mph in order to feel nature closely. Treating the arm as a 2-ft-long and 3-in-diameter cylinder, determine the drag force on both arms. *Answer:* 1.02 lbf
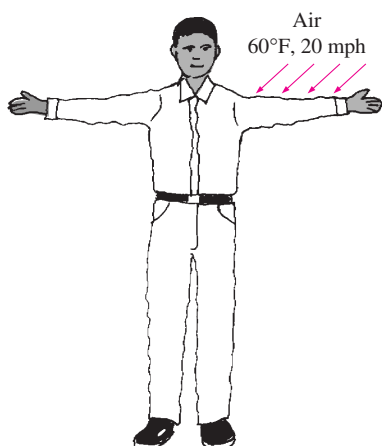
Air
60°F, 20 mph

FIGURE P15–64E

15–65 A 6-mm-diameter electrical transmission line is exposed to windy air. Determine the drag force exerted on a 120-m-long section of the wire during a windy day when the air is at 1 atm and 15°C and the wind is blowing across the transmission line at 40 km/h.

15–66 Consider 0.8-cm-diameter hail that is falling freely in atmospheric air at 1 atm and 5°C. Determine the terminal velocity of the hail. Take the density of hail to be 910 kg/m³.

15–67 A 0.1-mm-diameter dust particle whose density is 2.1 g/cm³ is observed to be suspended in the air at 1 atm and 25°C at a fixed point. Estimate the updraft velocity of air motion at that location. Assume the Stokes law to be applicable. Is this a valid assumption? *Answer:* 0.62 m/s

15–68 Dust particles of diameter 0.05 mm and density 1.8 g/cm³ are unsettled during high winds and rise to a height of 350 m by the time things calm down. Estimate how long it will take for the dust particles to fall back to the ground in air at 1 atm and 15°C, and their velocity. Disregard the initial transient period during which the dust particles accelerate to their terminal velocity, and assume Stokes law to be applicable.

15–69 A 2-m-long, 0.2-m-diameter cylindrical pine log (density = 513 kg/m³) is suspended by a crane
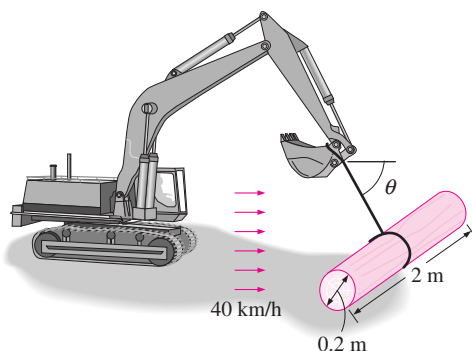
θ

2 m

40 km/h

0.2 m

FIGURE P15–69

in the horizontal position. The log is subjected to normal winds of 40 km/h at 5°C and 88 kPa. Disregarding the weight of the cable and its drag, determine the angle θ the cable will make with the horizontal and the tension on the cable.

15–70 One of the popular demonstrations in science museums involves the suspension of a ping-pong ball by an upward air jet. Children are amused by the ball always coming back to the center when it is pushed by a finger to the side of the jet. Explain this phenomenon using the Bernoulli equation. Also determine the velocity of air if the ball has a mass of 2.6 g and a diameter of 3.8 cm. Assume air is at 1 atm and 25°C.
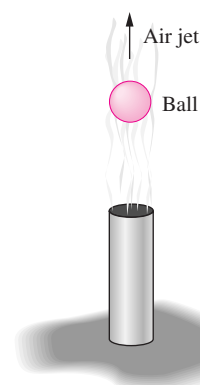
Air jet

Ball

FIGURE P15–70

Lift

15–71C Why is the contribution of viscous effects to lift usually negligible for airfoils?

15–72C Air is flowing past a symmetrical airfoil at zero angle of attack. Will the (*a*) lift and (*b*) drag acting on the airfoil be zero or nonzero?

15–73C Air is flowing past a nonsymmetrical airfoil at zero angle of attack. Will the (*a*) lift and (*b*) drag acting on the airfoil be zero or nonzero?

15–74C Air is flowing past a symmetrical airfoil at an angle of attack of 5°. Will the (*a*) lift and (*b*) drag acting on the airfoil be zero or nonzero?

15–75C What is stall? What causes an airfoil to stall? Why are commercial aircraft not allowed to fly at conditions near stall?

15–76C Both the lift and the drag of an airfoil increase with an increase in the angle of attack. In general, which increases at a much higher rate, the lift or the drag?

15–77C Why are flaps used at the leading and trailing edges of the wings of large aircraft during takeoff and landing? Can an aircraft take off or land without them?

15–78C How do the flaps affect the lift and the drag of the wings?

15–79C What is the effect of wing tip vortices (the air circulation from the lower part of the wings to the upper part) on the drag and the lift?

15–80C What is induced drag on wings? Can induced drag be minimized by using long and narrow wings or short and wide wings?

15–81C Air is flowing past a spherical ball. Will the lift exerted on the ball be zero or nonzero? Answer the same question if the ball is spinning.

15–82 A tennis ball with a mass of 57 g and a diameter of 6.4 cm is hit with an initial velocity of 92 km/h and a backspin of 4200 rpm. Determine if the ball will fall or rise under the combined effect of gravity and lift due to spinning shortly after hitting. Assume air is at 1 atm and 25°C.
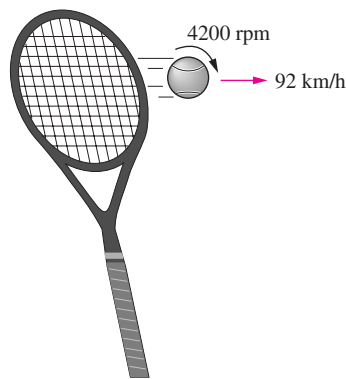

FIGURE P15–82

15–83 Consider an aircraft, which takes off at 190 km/h when it is fully loaded. If the weight of the aircraft is increased by 20 percent as a result of overloading, determine the speed at which the overloaded aircraft will take off. *Answer:* 208 km/h

15–84 Consider an airplane whose takeoff speed is 220 km/h and that takes 15 s to take off at sea level. For an airport at an elevation of 1600 m (such as Denver), determine (*a*) the takeoff speed, (*b*) the takeoff time, and (*c*) the additional runway length required for this airplane. Assume constant acceleration for both cases.
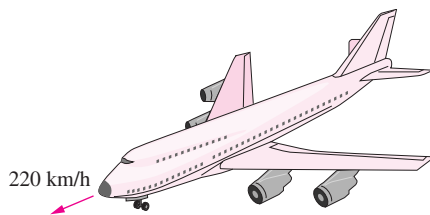

FIGURE P15–84

15–85E An airplane is consuming fuel at a rate of 5 gal/min when cruising at a constant altitude of 10,000 ft at constant speed. Assuming the drag coefficient to remain the same,

determine the rate of fuel consumption at an altitude of 30,000 ft at the same speed.

15–86 A jumbo jet airplane has a mass of about 400,000 kg when fully loaded with over 400 passengers and takes off at a speed of 250 km/h. Determine the takeoff speed when the airplane has 100 empty seats. Assume each passenger with luggage is 140 kg and the wing and flap settings are maintained the same. *Answer:* 246 km/h

15–87 Reconsider Prob. 15–86. Using EES (or other) software, investigate the effect of passenger count on the takeoff speed of the aircraft. Let the number of passengers vary from 0 to 500 in increments of 50. Tabulate and plot the results.

15–88 A small aircraft has a wing area of 30 m², a lift coefficient of 0.45 at takeoff settings, and a total mass of 2800 kg. Determine (*a*) the takeoff speed of this aircraft at sea level at standard atmospheric conditions, (*b*) the wing loading, and (*c*) the required power to maintain a constant cruising speed of 300 km/h for a cruising drag coefficient of 0.035.
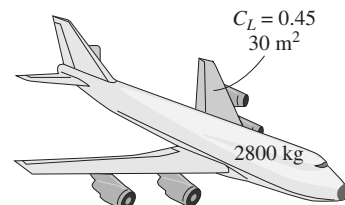

FIGURE P15–88

15–89 A small airplane has a total mass of 1800 kg and a wing area of 42 m². Determine the lift and drag coefficients of this airplane while cruising at an altitude of 4000 m at a constant speed of 280 km/h and generating 190 kW of power.

15–90 The NACA 64(l)–412 airfoil has a lift-to-drag ratio of 50 at 0° angle of attack, as shown in Fig. 15–42. At what angle of attack will this ratio increase to 80?

15–91 Consider a light plane that has a total weight of 15,000 N and a wing area of 46 m² and whose wings resemble the NACA 23012 airfoil with no flaps. Using data from Fig. 15–44, determine the takeoff speed at an angle of attack of 5° at sea level. Also determine the stall speed.
Answer: 94 km/h

15–92 An airplane has a mass of 50,000 kg, a wing area of 300 m², a maximum lift coefficient of 3.2, and a cruising drag coefficient of 0.03 at an altitude of 12,000 m. Determine (*a*) the takeoff speed at sea level, assuming it is 20 percent over the stall speed, and (*b*) the thrust that the engines must deliver for a cruising speed of 700 km/h.

15–93E A 2.4-in-diameter smooth ball rotating at 500 rpm is dropped in a water stream at 60°F flowing at 4 ft/s. Determine the lift and the drag force acting on the ball when it is first dropped in water.

Review Problems

15–94 An automotive engine can be approximated as a 0.4-m-high, 0.60-m-wide, and 0.7-m-long rectangular block. The ambient air is at 1 atm and 15°C. Determine the drag force acting on the bottom surface of the engine block as the car travels at a velocity of 85 km/h. Assume the flow to be turbulent over the entire surface because of the constant agitation of the engine block. *Answer:* 0.65 N
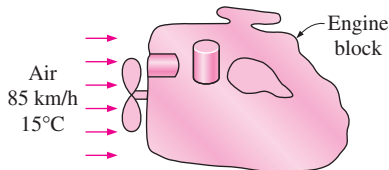

FIGURE P15–94

15–95 Calculate the thickness of the boundary layer during flow over a 2.5-m-long flat plate at intervals of 25 cm and plot the boundary layer over the plate for the flow of (*a*) air, (*b*) water, and (*c*) engine oil at 1 atm and 20°C at an upstream velocity of 3 m/s.

15–96E The passenger compartment of a minivan traveling at 60 mph in ambient air at 1 atm and 80°F can be modeled as a 3.2-ft-high, 6-ft-wide, and 11-ft-long rectangular box. The air flow over the exterior surfaces can be assumed to be turbulent because of the intense vibrations involved. Determine the drag force acting on the top and the two side surfaces of the van and the power required to overcome it.
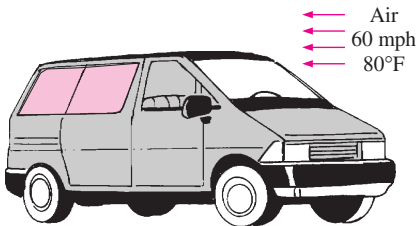

FIGURE P15–96E

15–97 A 1-m-external-diameter spherical tank is located outdoors at 1 atm and 25°C and is subjected to winds at 35 km/h. Determine the drag force exerted on it by the wind.
Answer: 3.5 N

15–98 A 2-m-high, 4-m-wide rectangular advertisement panel is attached to a 4-m-wide, 0.15-m-high rectangular concrete block (density = 2300 kg/m^3) by two 5-cm-diameter, 4-m-high (exposed part) poles, as shown in the figure. If the sign is to withstand 150 km/h winds from any direction, determine (*a*) the maximum drag force on the panel, (*b*) the drag force acting on the poles, and (*c*) the minimum length *L* of the concrete block for the panel to resist the winds. Take the density of air to be 1.30 kg/m^3.
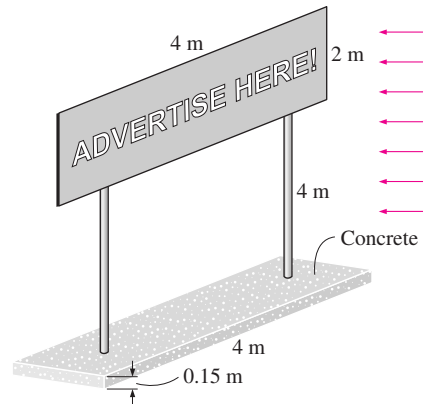

FIGURE P15–98

15–99 A plastic boat whose bottom surface can be approximated as a 1.5-m-wide, 2-m-long flat surface is to move through water at 15°C at speeds up to 30 km/h. Determine the friction drag exerted on the boat by water and the power needed to overcome it.
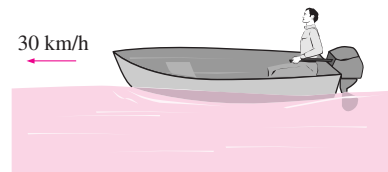

FIGURE P15–99

15–100 Reconsider Prob. 15–99. Using EES (or other) software, investigate the effect of boat speed on the drag force acting on the bottom surface of the boat, and the power needed to overcome it. Let the boat speed vary from 0 to 100 km/h in increments of 10 km/h. Tabulate and plot the results.

15–101E A commercial airplane has a total mass of 150,000 lbm and a wing planform area of 1800 ft^2. The plane has a cruising speed of 550 mph and a cruising altitude of 38,000 ft where the air density is 0.0208 lbm/ft^3. The plane has double-slotted flaps for use during takeoff and landing, but it cruises with all flaps retracted. Assuming the lift and drag characteristics of the wings can be approximated by NACA 23012, determine (*a*) the minimum safe speed for takeoff and landing with and without extending the flaps, (*b*) the angle of attack to cruise steadily at the cruising altitude, and (*c*) the power that needs to be supplied to provide enough thrust to overcome drag. Take the air density on the ground to be 0.075 lbm/ft^3.

15–102 An 8-cm-diameter smooth ball has a velocity of 36 km/h during a typical hit. Determine the percent increase in the drag coefficient if the ball is given a spin of 3500 rpm in air at 1 atm and 25°C.

15–103 A paratrooper and his 8-m-diameter parachute weigh 950 N. Taking the average air density to be 1.2 kg/m³, determine the terminal velocity of the paratrooper.
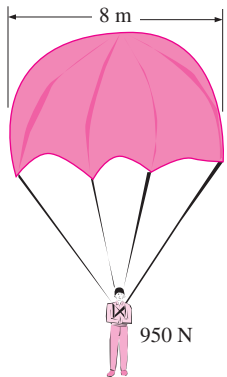*Answer:* 4.9 m/s

FIGURE P15–103

15–104 A 17,000-kg tractor-trailer rig has a frontal area of 9.2 m², a drag coefficient of 0.96, a rolling resistance coefficient of 0.05 (multiplying the weight of a vehicle by the rolling resistance coefficient gives the rolling resistance), a bearing friction resistance of 350 N, and a maximum speed of 110 km/h on a level road during steady cruising in calm weather with an air density of 1.25 kg/m³. Now a fairing is installed to the front of the rig to suppress separation and to streamline the flow to the top surface, and the drag coefficient is reduced to 0.76. Determine the maximum speed of the rig with the fairing.   *Answer:* 133 km/h

15–105 Stokes law can be used to determine the viscosity of a fluid by dropping a spherical object in it and measuring the terminal velocity of the object in that fluid. This can be done by plotting the distance traveled against time and observing when the curve becomes linear. During such an experiment a 3-mm-diameter glass ball ($\rho = 2500$ kg/m³) is dropped into a fluid whose density is 875 kg/m³, and the terminal velocity is measured to be 0.12 m/s. Determine the viscosity of the fluid.
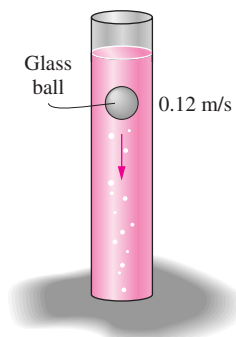

FIGURE P15–105

15–106 During an experiment, three aluminum balls ($\rho_s = 2600$ kg/m³) having diameters 2 mm, 4 mm, and 10 mm are dropped into a tank filled with glycerin at 22°C ($\rho_f = 1274$ kg/m³ and $\mu = 1$ kg/m · s). The terminal settling velocities of the balls are measured to be 3.2 mm/s, 12.8 mm/s, and 60.4 mm/s, respectively. Compare these values with the velocities predicted by Stokes law for drag force $F_D = 3\pi\mu D\mathcal{V}$, which is valid for very low Reynolds numbers (Re ≪ 1). Determine the error involved for each case, and assess the accuracy of Stokes law.

15–107 Repeat Prob. 15–106 by considering the general form of Stokes law expressed as $F_D = 3\pi\mu D\mathcal{V} + (9\pi/16)\rho_s\mathcal{V}^2 D^2$.

15–108 A small aluminum ball with $D = 2$ mm and $\rho_s = 2700$ kg/m³ is dropped into a large container filled with oil at 40°C ($\rho_f = 876$ kg/m³ and $\mu = 0.2177$ kg/m · s). The Reynolds number is expected to be low and thus Stroke's law for drag force $F_D = 3\pi\mu D\mathcal{V}$ to be applicable. Show that the variation of velocity with time can be expressed as $\mathcal{V} = \dfrac{a}{b}(1 - e^{-bt})$ where $a = g(1 - \rho_f/\rho_s)$ and $b = 18\mu/(\rho_s D^2)$. Plot the variation of velocity with time, and calculate the time it takes for the ball to reach 99 percent of its terminal velocity.

15–109 [ECS] Engine oil at 40°C is flowing over a long flat plate with a velocity of 4 m/s. Determine the distance x_{cr} from the leading edge of the plate where the flow becomes turbulent and calculate and plot the thickness of the boundary layer over a length of $2x_{\text{cr}}$.

Design and Essay Problems

15–110 Write a report on the history of the reduction of the drag coefficients of cars and obtain the drag coefficient data for some recent car models from the catalogs or car manufacturers.

15–111 Write a report on the flaps used at the leading and trailing edges of the wings of large commercial aircraft. Discuss how the flaps affect the drag and lift coefficients during takeoff and landing.

15–112 Large commercial airplanes cruise at high altitudes (up to about 40,000 ft) to save fuel. Discuss how flying at high altitudes reduces drag and saves fuel. Also discuss why small planes fly at relatively low altitudes.

15–113 Many drivers turn off their air conditioners and roll down the car windows in hopes of saving fuel. But it is claimed that this apparent "free cooling" actually increases the fuel consumption of the car. Investigate this matter and write a report on which practice will save gasoline under what conditions.